Laser cooling and trapping of atoms

H.J. Metcalf and P. van der Straten
Department of Physics, State University of New York,
Stony Brook, N.Y. 11794, U.S.A.
and
Debye Institute, Department of Atomic- and Interface Physics,
Utrecht University, P.O. Box 80.000,
3508 TA Utrecht, The Netherlands

I. INTRODUCTION

This article begins with some of the general ideas about laser cooling. One of the characteristics of optical control of atomic motion is that the speed of atoms can be considerably reduced. Since the spread of velocities of a sample of atoms is directly related to its temperature, the field has been dubbed laser cooling, and this name has persisted throughout the years.

In section II we introduce the general idea of optical forces and how they can act on atoms. We show how such forces can be velocity dependent, and thus non-conservative, which makes it possible to use optical forces for cooling. The section concludes with the discussion of a few special temperatures. Section III presents a quantum mechanical description of the origin of the force resulting from the atomic response to both stimulated and spontaneous emission processes. This is quite different from the familiar quantum mechanical calculations using state vectors to describe the state of the system, since spontaneous emission causes the state of the system to evolve from a pure state into a mixed state. Since spontaneous emission is an essential ingredient for the dissipative nature of the optical forces, the density matrix is introduced to describe it. The evolution of the density matrix is given by the optical Bloch equations (OBE), and the optical force is calculated from them. It is through the OBE that the dissipative aspects of laser cooling are introduced to the otherwise conservative quantum mechanics. The velocity dependence is treated as an extension of the force on an atom at rest.

In section IV the first modern laser cooling experiments are described. Atoms in beams were slowed down from thermal velocity to a few m/s, and the dominant problem was the change in Doppler shift arising from such a large change in velocity. Some typical values of parameters are discussed and tabulated. Section V introduces true cooling by optical forces to the μK regime. Such experiments require at least two laser beams, and are called optical molasses because the resulting viscous force can slow atoms to extremely slow velocities, and hence compress the width of the velocity distribution. The limits of such laser cooling are discussed, as well as the extension from experiments in 1D to 3D. Here the velocity dependence of the force is built into the description via the Doppler shift instead of being added in as an extension of the treatment. In 1988 some experiments reported temperatures below the limit calculated for optical molasses, and section VI presents the new description of laser cooling that emerged from this surprise. For the first time, the force resulting from spontaneous emission in combination with the multiple level structure of real atoms were embodied in the discussion. Here the new limits of laser cooling are presented.

The discussion up to this point has been on atomic velocities, and thus can be described in terms of a velocity space. Laser cooling thus collects atoms near the origin of velocity space. It is also possible to collect atoms into a small region of ordinary configuration space, and such trapping is discussed in section VII. Neutral atom traps can employ magnetic fields, optical fields, and both working together. However, such traps are always very shallow, and so only atoms that have been cooled to the few mK domain can be captured. The combination of laser cooling and atom trapping has produced astounding new tools for atomic physicists, and section VIII describes some of the applications and uses of these wonderful new capabilities.

II. GENERAL PROPERTIES CONCERNING LASER COOLING

These experiments almost always involve atomic absorption of nearly resonant light. The energy of the light $\hbar\omega$ raises the internal energy of the atom, and the angular momentum $\hbar$ changes the internal angular momentum ℓ of the electron, as described by the well-known selection rule $\Delta\ell = \pm 1$. By contrast, the linear momentum of the light $p = E/c = h/\lambda$ ($\vec{p} = \hbar\vec{k}$) cannot be absorbed by internal atomic degrees of freedom, and therefore must change the motion of the atoms in the laboratory frame. The force resulting from this momentum exchange between the light field and the atoms can be used in many ways to control atomic motion, and is the subject of this article.

Absorption of light populates the atomic excited state, and the return to the ground state can be either by spontaneous or by stimulated emission. The nature of the optical force that arises from these two different processes is quite different, and will be described separately. Such atomic transitions, *i.e.*, the motion of the atomic electrons, must be described quantum mechanically in the well-known form of the Schrödinger equation. By contrast, the center-of-mass motion of the atoms can usually be described classically, but there are many cases where even this is not possible so it must also involve quantum mechanics.

In the simplest possible case, the absorption of well-directed light from a laser beam, the momentum exchange between the light field and the atoms results in a force

$$\vec{F} = d\vec{p}/dt = \hbar\vec{k}\gamma_p, \tag{1}$$

where γ_p is the excitation rate of the atoms. The absorption leaves the atoms in their excited state, and if the light intensity is low enough so that they are much more likely to return to the ground state by spontaneous emission than by stimulated emission, the resulting fluorescent light carries off momentum $\hbar k$ in a random direction. The momentum exchange from the fluorescence averages zero, so the net total force is given by Eq. 1.

The scattering rate γ_p depends on the laser detuning from atomic resonance $\delta = \omega_\ell - \omega_a$, where ω_ℓ is the laser frequency and ω_a is the atomic resonance frequency. This detuning is measured in the atomic reference frame, and it is necessary that the Doppler-shifted laser frequency in the moving atoms' reference frame be used to calculate the absorption and scattering rate. Then γ_p is given by the Lorentzian

$$\gamma_p = \frac{s_0\gamma/2}{1 + s_0 + [2(\delta + \omega_D)/\gamma]^2}, \tag{2}$$

where $\gamma \equiv 1/\tau$ is an angular frequency corresponding to the decay rate of the excited state. Here $s_0 = I/I_s$ is the ratio of the light intensity I to the saturation intensity $I_s \equiv \pi hc/3\lambda^3\tau$, which is a few mW/cm^2 for typical atomic transitions (λ is the optical wavelength). The Doppler shift seen by the moving atoms is $\omega_D = -\vec{k}\cdot\vec{v}$ (note that $\vec{k}$ opposite to $\vec{v}$ produces a positive Doppler shift). The force is thus velocity-dependent, and the experimenter's task is to exploit this dependence to the desired goal, for example, optical friction for laser cooling.

The spontaneous emission events produce unpredictable changes in atomic momenta so the discussion of atomic motion must also include a "random walk" component. This can be described as a diffusion of the atomic momenta in momentum space, similar to Brownian motion in real space. The evolution of the momentum distribution in such circumstances is described by the Fokker-Planck equation, and it can be used for a more formal treatment of the laser cooling process. Solutions of the Fokker-Planck equation in limiting cases can ultimately be used to relate the velocity distribution of the atoms with their temperature.

The idea of "temperature" in laser cooling requires some careful discussion and disclaimers. In thermodynamics, temperature is carefully defined as a parameter of the state of a closed system in thermal equilibrium with its surroundings. This, of course, requires that there be thermal contact, *i.e.*, heat exchange, with the environment. In laser cooling this is clearly not the case because a sample of atoms is always absorbing and scattering light. Furthermore, there is essentially no heat exchange (the light cannot be considered as heat even though it is indeed a form of energy). Thus the system may very well be in a steady-state situation, but certainly not in thermal equilibrium, so that the assignment of a thermodynamic "temperature" is completely inappropriate.

Nevertheless, it is convenient to use the label of temperature to describe an atomic sample whose average kinetic energy $\langle E_k\rangle$ in one dimension has been reduced by the laser light, and this is written simply as $k_BT/2 = \langle E_k\rangle$, where k_B is Boltzmann's constant. It must be remembered that this temperature assignment is absolutely inadequate for atomic samples that do not have a Maxwell-Boltzmann velocity distribution, whether or not they are in thermal contact with the environment: there are infinitely many velocity distributions that have the same value of $\langle E_k\rangle$ but are so different from one another that characterizing them by the same "temperature" is a severe error.

With these ideas in mind, it is useful to define a few rather special values of temperatures associated with laser cooling. The highest of these temperatures corresponds to the energy associated with atoms whose speed and concomitant Doppler shift puts them just at the boundary of absorption of light. This velocity is $v_c \equiv \gamma/k \sim$ few m/s, and the corresponding temperature is $k_BT_c \equiv M\gamma^2/k^2$, and is typically several mK (here M is the atomic mass).

The next characteristic temperature corresponds to the energy associated with the natural width of atomic transitions, and is called the Doppler temperature. It is given

by $k_B T_D \equiv \hbar\gamma/2$. Because it corresponds to the limit of certain laser cooling processes, it is often called the Doppler limit, and is typically several hundred μK. Associated with this temperature is the one-dimensional velocity $v_D = \sqrt{k_B T_D/M} \sim 30$ cm/s.

The last of these three characteristic temperatures corresponds to the energy associated with a single photon recoil. In the absorption or emission process of a single photon, the atoms obtain a recoil velocity $v_r \equiv \hbar k/M$. The corresponding energy change can be related to a temperature, the recoil limit, defined as $k_B T_r \equiv \hbar^2 k^2/M$, and is generally regarded as the lower limit for optical cooling processes (although there are a few clever schemes that cool below it). It is typically a few μK, and corresponds to speeds of $v_r \sim 1$ cm/s.

These three temperatures are related to one another through a single dimensionless parameter $\varepsilon \equiv \omega_r/\gamma$ that is ubiquitous in describing laser cooling. It is the ratio of the recoil-frequency $\omega_r \equiv \hbar k^2/2M$ to the natural width γ, and as such embodies most of the important information that characterize laser cooling on a particular atomic transition. Typically $\varepsilon \sim 10^{-3}$ – 10^{-2}, and clearly $T_r = 4\varepsilon T_D = 4\varepsilon^2 T_c$.

In laser cooling and related aspects of optical control of atomic motion, the forces arise because of the exchange of momentum between the atoms and the laser field. Since the energy and momentum exchange is necessarily in discrete quanta rather than continuous, the interaction is characterized by finite momentum "kicks". This is often described in terms of "steps" in a fictitious space whose axes are momentum rather than position. These steps in momentum space are of size $\hbar k$ and thus are generally small compared to the magnitude of the atomic momenta at thermal velocities $\bar{v}$. This is easily seen by comparing $\hbar k$ with $M\bar{v}$,

$$\frac{\hbar k}{M\bar{v}} = \sqrt{\frac{T_r}{T}} \ll 1. \tag{3}$$

Thus the scattering of a single photon has a negligibly small effect on the motion of thermal atoms, but repeated cycles of absorption and emission can cause a large change of the atomic momenta and velocities.

III. THEORETICAL DESCRIPTION

A. Force on a two-level atom

We begin the calculation of the optical force on atoms by considering the simplest schemes, namely, a single-frequency light field interacting with a two-level atom confined to one dimension. It is based on the interaction of two-level atoms with a laser field as discussed in many textbooks [1].

The philosophy of the correspondence principle requires a smooth transition between quantum and classical mechanics. Thus the force F on an atom is defined as the expectation value of the quantum mechanical force-operator $\mathcal{F}$, as defined by $F = \langle \mathcal{F} \rangle = \mathrm{d} \langle p \rangle / \mathrm{d}t$. The time evolution of the expectation value of a time-independent quantum mechanical operator $\mathcal{A}$ is given by

$$\frac{\mathrm{d}}{\mathrm{d}t} \langle A \rangle = \frac{i}{\hbar} \langle [\mathcal{H}, \mathcal{A}] \rangle . \tag{4}$$

The commutator of $\mathcal{H}$ and p is given by $[\mathcal{H}, p] = i\hbar \, (\partial \mathcal{H}/\partial z)$, where the operator p has been replaced by $-i\hbar(\partial/\partial z)$. The force on an atom is then given by

$$F = - \left\langle \frac{\partial \mathcal{H}}{\partial z} \right\rangle . \tag{5}$$

This relation is a specific example of the Ehrenfest-theorem and forms the quantum mechanical analog of the classical expression that the force is the negative gradient of the potential.

Discussion of the force on atoms caused by light fields begins with that part of the Hamiltonian that describes the electric dipole interaction between the atom and the light field. The electric field of the light is written as $\vec{\mathcal{E}}(\vec{r}, t) = E_0 \hat{\epsilon} \cos(kz - \omega t)$ and the interaction Hamiltonian is $\mathcal{H}' = -e\vec{\mathcal{E}}(\vec{r}, t) \cdot \vec{r}$ where $\vec{r}$ is the electron coordinate. It has only off-diagonal matrix elements given by $\mathcal{H}'_{eg} = -eE_0 \hat{\epsilon} \cdot \langle e|\vec{r}|g\rangle$ where e and g represent the excited and ground states respectively. The force depends on the atomic state as determined by its interaction with the light, and is calculated from the expectation value $\langle \mathcal{A} \rangle = \mathrm{Tr}(\rho \mathcal{A})$, where ρ is the density matrix found by solving the optical Bloch equations (OBE) [1]. Then

$$F = \hbar \left(\frac{\partial \Omega}{\partial z} \rho^*_{eg} + \frac{\partial \Omega^*}{\partial z} \rho_{eg} \right) . \tag{6}$$

where the Rabi frequency is defined as $\hbar\Omega \equiv \mathcal{H}'_{eg}$. Note that the force depends on the state of the atom, and in particular, on the optical coherence between the ground and excited states, ρ_{eg}.

Although it may seem a bit artificial, it is instructive to split $\partial\Omega/\partial z$ into its real and imaginary parts (the matrix element that defines Ω can certainly be complex):

$$\frac{\partial \Omega}{\partial z} = (q_r + iq_i)\Omega. \tag{7}$$

Here $q_r + iq_i$ is the logarithmic derivative of Ω. In general, for a field $E(z) = E_0(z)\exp(i\phi(z)) + \text{c.c.}$, the real part of the logarithmic derivative corresponds to a gradient of the amplitude $E_0(z)$ and the imaginary part to a gradient of the phase $\phi(z)$. Then the expression for the force becomes

$$F = \hbar q_r(\Omega\rho^*_{eg} + \Omega^*\rho_{eg}) + i\hbar q_i(\Omega\rho^*_{eg} - \Omega^*\rho_{eg}). \tag{8}$$

Equation 8 is a very general result that can be used to find the force for any particular situation as long as the OBE for ρ_{eg} can be solved. In spite of the chosen complex expression for Ω, it is important to note that the force itself is real, and that the first term of the force is proportional to the real part of $\Omega\rho^*_{eg}$, whereas the second term is proportional to the imaginary part.

B. A Two-Level Atom at Rest

There are two important special optical arrangements to consider. The first one is a traveling wave whose electric field is $E(z) = (E_0/2)\left(e^{i(kz-\omega t)} + \text{c.c.}\right)$. In calculating the Rabi frequency from this, the rotating wave approximation (RWA) causes the positive frequency component of $E(z)$ to drop out. Then the gradient of the Rabi frequency becomes proportional to the gradient of the surviving negative frequency component, so that $q_r = 0$ and $q_i = k$. For such a traveling wave the amplitude is constant but the phase is not, and this leads to the nonzero value of q_i.

This is in direct contrast to the case of a standing wave, composed of two counterpropagating traveling waves so its amplitude is twice as large, for which the electric field is given by $E(z) = E_0 \cos(kz)\left(e^{-i\omega t} + \text{c.c.}\right)$, so that $q_r = -k\tan(kz)$ and $q_i = 0$. Again, only the negative frequency part survives the RWA, but the gradient does not depend on it. Thus a standing wave has an amplitude-gradient, but not a phase gradient.

The steady-state solutions of the OBE for a two-level atom at rest provide simple expressions for ρ [1]. Substituting the solution for ρ_{eg} into Eq. 8 gives

$$F = \frac{\hbar s}{1+s}\left(-\delta q_r + \frac{1}{2}\gamma q_i\right), \tag{9}$$

where $s \equiv s_0/[1+(2\delta/\gamma)^2]$ is the off-resonance saturation parameter. Note that the first term is proportional to the detuning δ, whereas the second term is proportional to the decay rate γ. For zero detuning, the force becomes $F = (\hbar k\gamma/2)[s_0/(s_0+1)]$, a very satisfying result because it is simply the momentum per photon $\hbar k$, times the scattering rate γ_p at resonance of Eq. 2.

It is instructive to identify the origin of both terms in Eq. 9. Absorption of light leads to the transfer of momentum from the optical field to the atoms. If the atoms decay by spontaneous emission, the recoil associated with the spontaneous fluorescence is in a random direction, so its average over many emission events results in zero net

effect on the atomic momentum. Thus the force from absorption followed by spontaneous emission can be written as $F_{\rm sp} = \hbar k \gamma \rho_{ee}$, where $\hbar k$ is the momentum transfer for each photon, γ is the rate for the process, and ρ_{ee} is the probability for the atoms to be in the excited state. Using Eq. 2, the force resulting from absorption followed by spontaneous emission becomes

$$F_{\rm sp} = \frac{\hbar k s_0 \gamma/2}{1 + s_0 + (2\delta/\gamma)^2}, \tag{10}$$

which saturates at large intensity as a result of the term s_0 in the denominator. Increasing the rate of absorption by increasing the intensity does not increase the force without limit, since that would only increase the rate of stimulated emission, where the transfer of momentum is opposite in direction compared to the absorption. Thus the force saturates to a maximum value of $\hbar k\gamma/2$, because ρ_{ee} has a maximum value of $1/2$.

Examination of Eq. 10 shows that it clearly corresponds to the second term of Eq. 8. This term is called the light pressure force, radiation pressure force, scattering-force, or dissipative force, since it relies on the scattering of light out of the laser beam. It vanishes for an atom at rest in a standing wave where $q_i = 0$, and this can be understood because atoms can absorb light from either of the two counterpropagating beams that make up the standing wave, and the average momentum transfer then vanishes. This force is dissipative because the reverse of spontaneous-emission is not possible, and therefore the action of the force cannot be reversed. It plays a very important role in the slowing and cooling of atoms.

By contrast, the first term in Eq. 8 derives from the light-shifts of the ground and excited states that depend on the strength of the optical electric field. A standing wave is composed of two counterpropagating laser beams, and their interference produces an amplitude gradient that is not present in a traveling wave. The force is proportional to the gradient of the light shift, and the ground-state light shift $\Delta E_g = \hbar\Omega^2/4\delta$ can be used to find the force on ground-state atoms in low intensity light:

$$F_{\rm dip} = -\frac{\partial(\Delta E_g)}{\partial z} = \frac{\hbar\Omega}{2\delta}\frac{\partial\Omega}{\partial z}. \tag{11}$$

For an amplitude-gradient light field such as a standing wave, $\partial\Omega/\partial z = q_r\Omega$, and this force corresponds to the first term in Eq. 8 in the limit of low saturation ($s \ll 1$).

For the case of a standing wave Eq. 9 becomes

$$F_{\rm dip} = \frac{2\hbar k\delta s_0 \sin 2kz}{1 + 4s_0\cos^2 kz + (2\delta/\gamma)^2}, \tag{12}$$

where s_0 is the saturation parameter of each of the two beams that form the standing wave. For $\delta < 0$ the force drives the atoms to positions where the intensity has a maximum, whereas for $\delta > 0$ the atoms are attracted to the intensity minima. The force is conservative and therefore cannot be used for cooling. This is called the dipole-force, reactive force, gradient force, or redistribution force. It has the same origin as the force of an inhomogeneous dc electric field on a classical dipole, but relies on the redistribution of photons from one laser beam to the other.

It needs to be emphasized that the forces of Eqs. 10 and 12 are two fundamentally different kinds of forces. For an atom at rest, the scattering force vanishes for a standing wave, whereas the dipole force vanishes for a traveling wave. The scattering force is dissipative, and can be used to cool, whereas the dipole force is conservative, and can be used to trap. Dipole forces can be made large by using high intensity light because they do not saturate. However, since the forces are conservative, they cannot be used to cool a sample of atoms. Nevertheless, they can be combined with the dissipative scattering force to enhance cooling in several different ways. By contrast, scattering forces are always limited by the rate of spontaneous emission γ and cannot be made arbitrarily strong, but they are dissipative and are required for cooling.

C. Atoms in Motion

Laser cooling requires dissipative or velocity-dependent forces that cannot be conservative. The procedure followed here is to treat the velocity of the atoms as a small perturbation, and make first-order corrections to the solutions of the OBE obtained for atoms at rest [2]. It begins by adding drift terms in the expressions for the relevant quantities. Thus the Rabi frequency satisfies

$$\frac{{\rm d}\Omega}{{\rm d}t} = \frac{\partial\Omega}{\partial t} + v\frac{\partial\Omega}{\partial z} = \frac{\partial\Omega}{\partial t} + v(q_r + iq_i)\Omega, \tag{13}$$

where Eq. 7 has been used to separate the gradient of Ω into real and imaginary parts. Differentiating the steady state density matrix elements found by solving the OBE [1] leads to

$$\frac{{\rm d}w}{{\rm d}t} = \frac{\partial w}{\partial t} + v\frac{\partial w}{\partial z} = \frac{\partial w}{\partial t} - \frac{2vq_r s}{(1+s)^2}, \tag{14}$$

since $s_0 = 2|\Omega|^2/\gamma^2$ and Ω depends on z. Here $w \equiv \rho_{gg} - \rho_{ee}$. Similarly,

$$\frac{{\rm d}\rho_{eg}}{{\rm d}t} = \frac{\partial\rho_{eg}}{\partial t} + v\frac{\partial\rho_{eg}}{\partial z} = \frac{\partial\rho_{eg}}{\partial t} - \frac{iv\Omega}{2(\gamma/2 - i\delta)(1+s)}\left[q_r\left(\frac{1-s}{1+s}\right) + \right. \tag{15}$$

Since neither w nor ρ_{eg} is explicitly time dependent, both $\partial w/\partial t$ and $\partial\rho_{eg}/\partial t$ vanish. The Eqs. 14 and 15 are still difficult to solve analytically for a general optical field, and the results are not very instructive. However, the solution for the two special cases of the standing and traveling waves provide considerable insight.

For a traveling wave $q_r = 0$, and the velocity-dependent force can be found by combining Eqs. 14

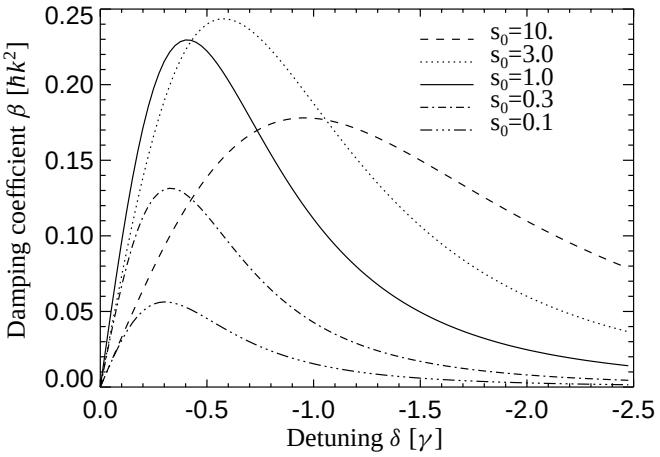

FIG. 1: The damping coefficient β for an atom in a traveling wave as a function of the detuning for different values of the saturation parameter s_0. The damping coefficient is maximum for intermediate detunings and intensities.

and 15 with the OBE to eliminate the time derivatives. The resulting coupled equations can be separated and substituted into Eq. 8 for the force to find, after considerable algebra,

$$F = \hbar q_i \, \frac{s\gamma/2}{1+s} \left(1 + \frac{2\delta v q_i}{(1+s)(\delta^2 + \gamma^2/4)} \right) \equiv F_0 - \beta v. \tag{16}$$

The first term is the velocity-independent force F_0 for an atom at rest given by Eq. 9. The second term is velocity-dependent and can lead to compression of the velocity distribution. For a traveling wave $q_i = k$ and thus the damping-coefficient β is given by

$$\beta = -\hbar k^2 \frac{4 s_0 (\delta/\gamma)}{(1 + s_0 + (2\delta/\gamma)^2)^2}. \tag{17}$$

Such a force can compress the velocity distribution of an atomic sample for negative values of δ, *i.e.*, for red detuned light. For small detuning and low intensity the damping coefficient β is linear in both parameters. However, for detunings much larger than γ and intensities much larger than I_s, β saturates and even decreases as a result of the dominance of δ in the denominator of Eq. 17. This behavior can be seen in Fig. 1, where the damping-coefficient β has been plotted as a function of detuning for different saturation parameters. The decrease of β for large detunings and intensities is caused by saturation of the transition, in which case the absorption rate becomes only weakly dependent on the velocity. The maximum value of β is obtained for $\delta = -\gamma/2$ and $s_0 = 2$, and is given by $\beta_{\max} = \hbar k^2/4$. The damping-rate Γ is given by $\Gamma \equiv \beta/M$, and its maximum value is $\Gamma_{\max} = \omega_r/2$, where ω_r is the recoil-frequency. For the alkalis this rate is of the order of 10^4–10^5 s^{-1}, indicating that atomic velocity distributions can be compressed in about 10-100 μs. Furthermore, F_0 in Eq. 16 is always present and so the atoms are *not* damped toward any constant velocity.

For a standing wave $q_i = 0$, and just as above, the velocity-dependent force can be found by combining Eqs. 14 and 15 with the OBE to eliminate the time derivatives. The resulting coupled equations can again be separated and substituted into Eq. 8 for the force to find

$$F = -\hbar q_r \, \frac{s\delta}{1+s} \left(1 - v q_r \, \frac{(1-s)\gamma^2 - 2s^2(\delta^2 + \gamma^2/4)}{(\delta^2 + \gamma^2/4)(1+s)^2 \gamma} \right), \tag{18}$$

where $q_r = -k \tan(kz)$. In the limit of $s \ll 1$, this force is

$$F = \hbar k \, \frac{s_0 \delta \gamma^2}{2(\delta^2 + \gamma^2/4)} \left(\sin 2kz + kv \frac{\gamma}{(\delta^2 + \gamma^2/4)} (1 - \cos 2kz) \right). \tag{19}$$

Here s_0 is the saturation parameter of each of the two beams that compose the standing wave. The first term is the velocity-independent part of Eq. 9 and is sinusoidal in space, with a period of $\lambda/2$. Thus its spatial average vanishes. The force remaining after such averaging is $F_{\rm av} = -\beta v$, where the damping coefficient β is given by

$$\beta = -\hbar k^2 \frac{8 s_0 (\delta/\gamma)}{(1 + (2\delta/\gamma)^2)^2}. \tag{20}$$

In contrast to the traveling-wave case, this is a true damping force because there is no F_0, so atoms are slowed toward $v = 0$ independent of their initial velocities. Note that this expression for β is valid only for $s \ll 1$ because it depends on spontaneous emission to return atoms to their ground state.

There is an appealing description of the mechanism for this kind of cooling in a standing wave. With light detuned below resonance, atoms traveling toward one laser beam see it Doppler shifted upward, closer to resonance. Since such atoms are traveling away from the other laser beam, they see its light Doppler shifted further downward, hence further out of resonance. Atoms therefore scatter more light from the beam counterpropagating to their velocity so their velocity is reduced. This damping mechanism is called optical-molasses, and is one of the most important tools of laser cooling.

Needless to say, such a pure damping force would reduce the atomic velocities, and hence the absolute temperature, to zero. Since this violates thermodynamics, there must be something left out of the description. It is the discreteness of the momentum changes in each case, $\Delta p = \hbar k$, that results in a minimum velocity change. The consequences of this discreteness can be described as a diffusion of the atomic momenta in momentum space by finite steps as discussed earlier.

D. The Fokker-Planck Equation

The random walk in momentum space associated with spontaneous emission is similar to Brownian motion in

coordinate space. There is an analogous momentum diffusion constant D, and so the atomic motion in momentum space can be described by the Fokker-Planck equation

$$\frac{\partial W(p,t)}{\partial t} = -\frac{\partial\left[F(p,t)W(p,t)\right]}{\partial p} + \frac{\partial^2\left[D(p,t)W(p,t)\right]}{\partial p^2} \tag{21}$$

where $W(p,t)$ is the momentum distribution of the atoms. For the special case when both the force and the diffusion are independent of time, the formal stationary solution is

$$\overline{W}(p) = \frac{C}{D(p)} \exp\left(\int_0^p \frac{F(p')}{D(p')} \mathrm{d}p'\right), \tag{22}$$

where C is an integration constant. Once the force and diffusion are known, the stationary solution of the Fokker-Planck equation emerges easily.

In the simplest and most common case in laser cooling the force is proportional to the velocity and the diffusion is independent of velocity:

$$F(v) = -\beta v \quad \text{and} \quad D(v) = D_0. \tag{23}$$

Then the stationary solution of Eq. **??** for $\overline{W}(v)$ is

$$\overline{W}(p) \propto e^{-\beta p^2/2MD_0}. \tag{24}$$

This is indeed a Maxwell-Boltzmann-distribution. For low intensity where spontaneous emission dominates, $D_0 = s\gamma(\hbar k)^2/2$, so the steady state temperature is given by $k_B T = D_0/\beta = \hbar\gamma/2$ for $\delta = -\gamma/2$, its optimum value [1]. This is called the Doppler temperature because the velocity dependence of the cooling mechanism derives from the Doppler shift. The fact that the conditions of Eqs. **??** for the force and diffusion are often approximately correct explains why the notion of temperature often appears as a description of a laser-cooled sample.

One of the most important properties of laser cooling is its ability to change the phase space density of an atomic sample. Changing the phase space density provides a most important distinction between light optics and atom optics. The Hamiltonian description of geometrical-optics leads to the brightness-theorem, that can be found in many optics books. Thus bundles of light rays obey a similar phase space density conservation. But there is a fundamental difference between light and atom optics. In the first case, the "forces" that determine the behavior of bundles of rays are "conservative" and phase space density is conserved. For instance, a lens can be used to focus a light beam to a small spot; however, at the same time the divergence of the beam must be increased, thus conserving phase space density. By contrast, in atom-optics dissipative forces that are velocity dependent can be used, and thus phase space density is no longer conserved. Optical elements corresponding to such forces can not exist for light, but in addition to the atom optic elements of lenses, collimators and others, phase space compressors can also be built. Such compression is essential in a large number of cases, such as atomic beam brightening for collision studies or cooling for the achievement of Bose-Einstein condensation.

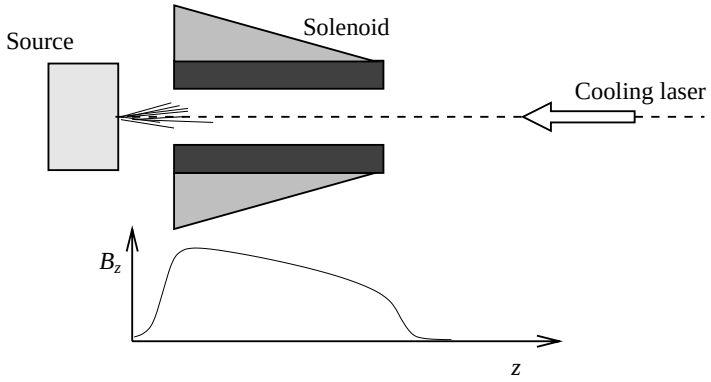

FIG. 2: Schematic diagram of apparatus for beam slowing. The tapered magnetic field is produced by layers of varying length on the solenoid. A plot of B_z *vs.* z is also shown.

atom	$T_{\rm oven}$ (K)	$\overline{v}$ (m/s)	$L_{\rm min}$ (m)	$t_{\rm min}$ (ms)
H	1000	5000	0.012	0.005
He*	4	158	0.03	0.34
He*	650	2013	4.4	4.4
Li	1017	2051	1.15	1.12
Na	712	876	0.42	0.96
K	617	626	0.77	2.45
Rb	568	402	0.75	3.72
Cs	544	319	0.93	5.82

TABLE I: Parameters of interest for slowing various atoms. The stopping length $L_{\rm min}$ and time $t_{\rm min}$ are minimum values. The oven temperature $T_{\rm oven}$ that determines the peak velocity is chosen to give a vapor pressure of 1 Torr. Special cases are H at 1000 K and He in the metastable triplet state, for which two rows are shown: one for a 4 K source and another for the typical discharge temperature.

IV. SLOWING ATOMIC BEAMS

Among the earliest laser cooling experiments was deceleration of atoms in a beam [3]. The authors exploited the Doppler-shift to make the momentum exchange (hence the force) velocity dependent. It worked by directing a laser beam opposite to an atomic beam so the atoms could absorb light, and hence momentum $\hbar k$, very many times along their paths through the apparatus as shown in Fig. 2 [3, 4]. Of course, excited-state atoms cannot absorb light efficiently from the laser that excited them, so between absorptions they must return to the ground state by spontaneous decay, accompanied by emission of fluorescent light. The spatial symmetry of the emitted fluorescence results in an average of zero net momentum transfer from many such fluorescence events. Thus the net force on the atoms is in the direction of the laser beam, and the maximum deceleration is limited by the spontaneous emission rate γ.

The maximum attainable deceleration is obtained for very high light intensities, and is limited because the atom must then divide its time equally between ground and excited states. High-intensity light can produce faster absorption, but it also causes equally fast stimulated-emission; the combination produces neither deceleration nor cooling because the momentum transfer to the atom in emission is then in the opposite direction to what it was in absorption. The force is limited to $F = \hbar k \gamma_p$, and so the deceleration therefore saturates at a value $\vec{a}_{\rm max} = \hbar \vec{k} \gamma / 2M$ (see Eq. 2). Since the maximum deceleration $\vec{a}_{\rm max}$ is fixed by atomic parameters, it is straightforward to calculate the minimum stopping length $L_{\rm min}$ and time $t_{\rm min}$ for the rms velocity of atoms $\bar{v} = 2\sqrt{k_B T/M}$ at the chosen temperature. The result is $L_{\rm min} = \overline{v}^2/2a_{\rm max}$ and $t_{\rm min} = \overline{v}/a_{\rm max}$. In Table I are some of the parameters for slowing a few atomic species of interest from the peak of the thermal velocity distribution.

Maximizing the scattering rate γ_p requires $\delta = -\omega_D$ in Eq. 2. If δ is chosen for a particular atomic velocity in the beam, then as the atoms slow down, their changing Doppler-shift will take them out of resonance. They will eventually cease deceleration after their Doppler shift has been decreased by a few times the power-broadened width $\gamma' = \gamma\sqrt{1+s_0}$, corresponding to Δv of a few times γ'/k. Although this Δv of a few m/s is considerably larger than the typical atomic recoil velocity $\hbar k/M$ of a few cm/s, it is still only a small fraction of the atoms' average thermal velocity $\overline{v}$, so that significant further cooling or deceleration cannot be accomplished.

In order to achieve deceleration that changes the atomic speeds by hundreds of m/s, it is necessary to maintain $(\delta + \omega_D) \ll \gamma$ by compensating such large changes of the Doppler-shift. This can be done by changing ω_D, or δ via either ω_ℓ or ω_a. The two most common methods for maintaining this resonance are sweeping the laser frequency ω_ℓ along with the changing ω_D of the decelerating atoms [5–7], or by spatially varying the atomic resonance frequency with an inhomogeneous dc magnetic field to keep the decelerating atoms in resonance with the fixed frequency laser [1, 3, 8].

The use of a spatially varying magnetic field to tune the atomic levels along the beam path was the first method to succeed in slowing atoms [3]. It works as long as the Zeeman shifts of the ground and excited states are different so that the resonant frequency is shifted. The field can be tailored to provide the appropriate Doppler-shift along the moving atom's path. For uniform deceleration $a \equiv \eta a_{\rm max}$ from initial velocity v_0, the appropriate field profile is $B(z) = B_0\sqrt{1 - z/z_0}$, where $z_0 \equiv Mv_0^2/\eta\hbar k\gamma$ is the length of the magnet, $B_0 = \hbar k v_0/\mu'$, $\mu' \equiv (g_e M_e - g_g M_g)\mu_B$, subscripts g and e refer to ground and excited states, $g_{g,e}$ is the Land"e-g-factor, μ_B is the Bohr magneton, and $M_{g,e}$ is the magnetic quantum number. The design parameter $\eta < 1$ determines the length of the magnet z_0. A solenoid that can produce such a spatially varying field has layers of decreasing lengths as shown schematically in Fig. 2. The techni-

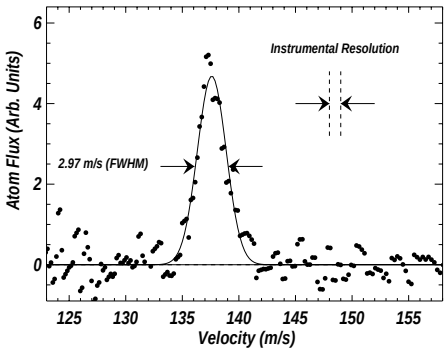

FIG. 3: The velocity distribution measured with the TOF method. The experimental width of approximately $\frac{1}{6}(\gamma/k)$ is shown by the dashed vertical lines between the arrows. The Gaussian fit through the data yields a FWHM of 2.97 m/s (figure from Ref. [10]).

cal problem of extracting the beam of slow atoms from the end of the solenoid can be simplified by reversing the field gradient and choosing a transition whose frequency decreases with increasing field [9].

For alkali atoms such as Na, a time-of-flight (TOF) method can be used to measure the velocity distribution of atoms in the beam. It employs two additional beams labeled pump and probe from laser 1 as shown in Fig. 2. Because these beams cross the atomic beam at 90°, $\omega_D = -\vec{k} \cdot \vec{v} = 0$ and they excite atoms at all velocities. The pump beam is tuned to excite and empty a selected ground hyperfine state (hfs), and it transfers more than 98% of the population as the atoms pass through its 0.5 mm width. To measure the velocity distribution of atoms in the selected hfs, this pump laser beam is interrupted for a period $\Delta t = 10 - 50$ μs with an acoustic optical modulator (AOM). A pulse of atoms in the selected hfs passes the pump region and travels to the probe beam. The time dependence of the fluorescence induced by the probe laser, tuned to excite the selected hfs, gives the time of arrival, and this signal is readily converted to a velocity distribution. Figure **??** shows the measured velocity distribution of the atoms slowed by laser 2.

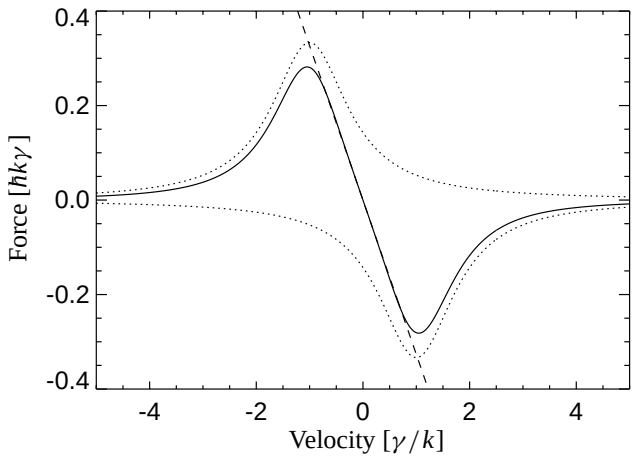

FIG. 4: Velocity dependence of the optical damping forces for one-dimensional optical molasses. The two dotted traces show the force from each beam, and the solid curve is their sum. The straight line shows how this force mimics a pure damping force over a restricted velocity range. These are calculated for $s_0 = 2$ and $\delta = -\gamma$ so there is some power broadening evident.

V. OPTICAL MOLASSES

A. Doppler Cooling

In Section III C above there was a discussion of the radiative force on atoms moving in a standing wave (counterpropagating laser beams). The slowing force is proportional to velocity for small enough velocities, resulting in viscous damping [11, 12] that gives this technique the name "optical molasses" (OM). By using three intersecting orthogonal pairs of oppositely directed beams, the movement of atoms in the intersection region can be severely restricted in all three dimensions, and many atoms can thereby be collected and cooled in a small volume. OM has been demonstrated at several laboratories [13], often with the use of low cost diode lasers [14].

It is straightforward to estimate the force on atoms in OM from Eq. 10. The discussion here is limited to the case where the light intensity is low enough so that stimulated-emission is not important. In this low intensity case the forces from the two light beams are simply added to give $\vec{F}_{OM} = \vec{F}_+ + \vec{F}_-$, where

$$\vec{F}_\pm = \pm\frac{\hbar\vec{k}\gamma}{2}\frac{s_0}{1+s_0+\left[2(\delta\mp|\omega_D|)/\gamma\right]^2}. \qquad (25)$$

Then the sum of the two forces is

$$\vec{F}_{OM} \cong \frac{8\hbar k^2\delta s_0\vec{v}}{\gamma(1+s_0+(2\delta/\gamma)^2)^2} \equiv -\beta\vec{v}, \qquad (26)$$

where terms of order $(kv/\gamma)^4$ and higher have been neglected (see Eq. 20).

These forces are plotted in Fig. 4. For $\delta < 0$, this force opposes the velocity and therefore viscously damps the atomic motion. $\vec{F}_{OM}$ has maxima near $v \approx \pm\gamma'/2k$ and decreases rapidly for larger velocities.

If there were no other influence on the atomic motion, all atoms would quickly decelerate to $v = 0$ and the sample would reach $T = 0$, a clearly unphysical result. There is also some heating caused by the light beams that must be considered, and it derives from the discrete size of the momentum steps the atoms undergo with each emission or absorption as discussed above for Brownian motion (see Sec. III D). Since the atomic momentum changes by $\hbar k$, their kinetic energy changes on the average by at least the recoil-energy $E_r = \hbar^2k^2/2M = \hbar\omega_r$. This means that the average frequency of each absorption is $\omega_{\rm abs} = \omega_a + \omega_r$ and the average frequency of each emission is $\omega_{\rm emit} = \omega_a - \omega_r$. Thus the light field loses an average energy of $\hbar(\omega_{\rm abs} - \omega_{\rm emit}) = 2\hbar\omega_r$ for each scattering. This loss occurs at a rate $2\gamma_p$ (two beams), and the energy is converted to atomic kinetic energy because the atoms recoil from each event. The atomic sample is thereby heated because these recoils are in random directions.

The competition between this heating with the damping force of Eq. 26 results in a nonzero kinetic energy in steady state where the rates of heating and cooling are equal. Equating the cooling rate, $\vec{F}\cdot\vec{v}$, to the heating rate, $4\hbar\omega_r\gamma_p$, the steady-state kinetic energy is $(\hbar\gamma/8)(2|\delta|/\gamma + \gamma/2|\delta|)$. This result is dependent on $|\delta|$, and it has a minimum at $2|\delta|/\gamma = 1$, whence $\delta = -\gamma/2$. The temperature found from the kinetic energy is then $T_D = \hbar\gamma/2k_B$, where k_B is Boltzmann's constant and T_D is called the Doppler temperature or the Doppler cooling limit. For ordinary atomic transitions, T_D is typically below 1 mK.

Another instructive way to determine T_D is to note that the average momentum transfer of many spontaneous emissions is zero, but the rms scatter of these about zero is finite. One can imagine these decays as causing a random-walk in momentum space with step size $\hbar k$ and step frequency $2\gamma_p$, where the factor of 2 arises because of the two beams. The random walk results in diffusion in momentum space with diffusion-coefficient $D_0 \equiv 2(\Delta p)^2/\Delta t = 4\gamma_p(\hbar k)^2$as discussed in Sec. III D. Then Brownian motion theory gives the steady-state temperature in terms of the damping coefficient β to be $k_BT = D_0/\beta$. This turns out to be $\hbar\gamma/2$ as above for the case $s_0 \ll 1$ when $\delta = -\gamma/2$. This remarkable result predicts that the final temperature of atoms in OM is independent of the optical wavelength, atomic mass, and laser intensity (as long as it is not too large).

B. Atomic Beam Collimation - One Dimensional Optical Molasses

When an atomic beam crosses a one-dimensional OM as shown in Fig. 5, the transverse motion of the atoms is quickly damped while the longitudinal component is essentially unchanged. This transverse cooling of an atomic

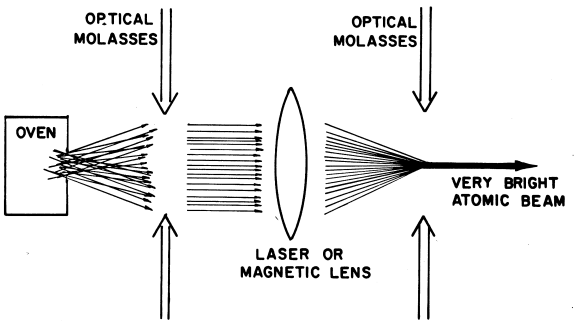

FIG. 5: Scheme for optical brightening of an atomic beam. First the transverse velocity components of the atoms are damped out by an optical molasses, then the atoms are focused to a spot, and finally the atoms are recollimated in a second optical molasses (figure from Ref. [15]).

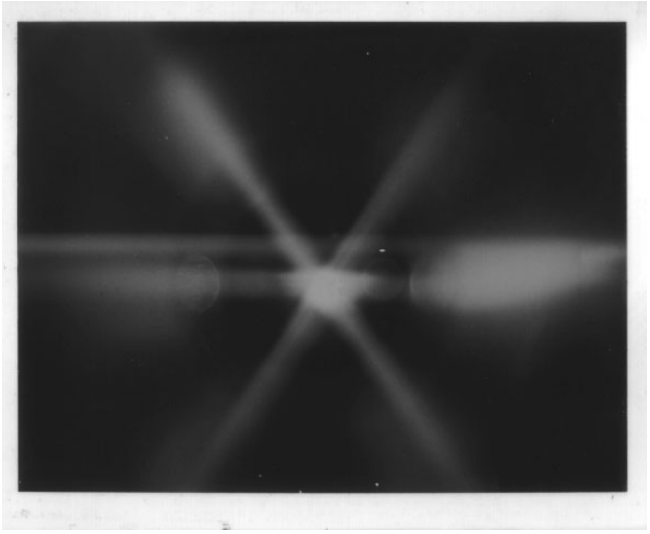

FIG. 6: Photograph of optical molasses in Na taken under ordinary snapshot conditions in the lab at NIST. The upper horizontal streak is from the slowing laser while the three beams that cross at the center are on mutually orthogonal axes viewed from the (111) direction. Atoms in the optical molasses glow brightly at the center (figure from Ref. [18]).

beam is an example of a method that can actually increase its brightness (atoms/sec-sr-cm^2) because such active collimation uses dissipative forces to compress the phase space volume occupied by the atoms. By contrast, the usual realm of beam focusing or collimation techniques for light beams and most particle beams, is restricted to selection by apertures or conservative forces that preserve the phase space density of atoms in the beam.

This velocity-compression at low intensity in one dimension can be simply estimated for two-level atoms in 1-D to be about $v_c/v_D = \sqrt{\gamma/\omega_r} = \sqrt{1/\varepsilon}$. For Rb, $v_D = 12$ cm/s, $v_c = \gamma/k \simeq 4.6$ m/s, $\omega_r \simeq 2\pi \times 3.8$ kHz, and $1/\varepsilon \simeq 1600$. Including two transverse directions along with the longitudinal slowing and cooling discussed above, the decrease in phase space volume from the momentum contribution alone for laser cooling of a Rb atomic beam can exceed 10^6.

Clearly optical techniques can create atomic beams enormously more times intense than ordinary thermal beams, and also many orders of magnitude brighter. Furthermore, this number could be increased several orders of magnitude if the transverse cooling could produce temperatures below the Doppler temperature. For atoms cooled to the recoil temperature $T_r = \hbar\omega_r/k_B$ where $\Delta p = \hbar k$ and $\Delta x = \lambda/\pi$, the brightness increase could be 10^{17}.

C. Experiments in Three-Dimensional Optical Molasses

Optical molasses experiments can also work in three dimensions at the intersection of three mutually orthogonal pairs of opposing laser beams (see Fig. 6). Even though atoms can be collected and cooled in the intersection region, it is important to stress again that this is *not* a trap. That is, atoms that wander away from the center experience no force directing them back. They are allowed to diffuse freely and even escape, as long as there is enough time for their very slow diffusive movement to allow them to reach the edge of the region of the intersection of the laser beams. Because the atomic velocities are randomized during the damping time $M/\beta = 2/\omega_r$, atoms execute a random-walk with a step size of $2v_D/\omega_r = \lambda/\pi\sqrt{2\varepsilon} \cong$ few μm. To diffuse a distance of 1 cm requires about 10^7 steps or about 30 s [16, 17].

Three-dimensional OM was first observed in 1985 [12]. Preliminary measurements of the average kinetic energy of the atoms were done by blinking off the laser beams for a fixed interval. Comparison of the brightness of the fluorescence before and after the turnoff was used to calculate the fraction of atoms that left the region while it was in the dark. The dependence of this fraction on the duration of the dark interval was used to estimate the velocity distribution and hence the temperature. The result was not inconsistent with the two level atom theory described above.

A few months later a more sensitive ballistic technique was devised at NIST that showed the astounding result that the temperature of the atoms in OM was very much lower than T_D [19]. These experiments also found that OM was less sensitive to perturbations and more tolerant of alignment errors than was predicted by the 1D, two-level atom theory. For example, if the intensities of the two counterpropagating laser beams forming an OM were unequal, then the force on atoms at rest would not vanish, but the force on atoms with some nonzero drift velocity *would* vanish. This drift velocity can be easily calculated by using Eq. 25 with unequal intensities s_{0+}

and s_{0-}, and following the derivation of Eq. 26. Thus atoms would drift out of an OM, and the calculated rate would be much faster than observed by deliberately unbalancing the beams in the experiments [13].

It was an enormous surprise to observe that the ballistically measured temperature of the Na atoms was as much as 10 times *lower* than $T_D = 240$ μK [19], the temperature minimum calculated from the theory. This breaching of the Doppler limit forced the development of an entirely new picture of OM that accounts for the fact that in 3D, a two-level picture of atomic structure is inadequate. The multilevel structure of atomic states, and optical pumping among these sublevels, must be considered in the description of 3D OM, as discussed below.

VI. COOLING BELOW THE DOPPLER LIMIT

A. Introduction

In response to the surprising measurements of temperatures below T_D, two groups developed a model of laser cooling that could explain the lower temperatures [20, 21]. The key feature of this model that distinguishes it from the earlier picture was the inclusion of the multiplicity of sublevels that make up an atomic state (*e.g.*, Zeeman and hfs). The dynamics of optically pumping atoms among these sublevels provides the new mechanism for producing the ultra-low temperatures [18].

The dominant feature of these models is the non-adiabatic response of moving atoms to the light field. Atoms at rest in a steady state have ground state orientations caused by optical-pumping processes that distribute the populations over the different ground-state sublevels. In the presence of polarization gradients, these orientations reflect the local light field. In the low-light-intensity regime, the orientation of stationary atoms is completely determined by the ground-state distribution: the optical coherences and the exited-state population follow the ground-state distribution adiabatically.

For atoms moving in a light field that varies in space, optical-pumping acts to adjust the atomic orientation to the changing conditions of the light field. In a weak pumping process, the orientation of moving atoms always lags behind the orientation that would exist for stationary atoms. It is this phenomenon of non-adiabatic following that is the essential feature of the new cooling process.

Production of spatially dependent optical-pumping processes can be achieved in several different ways. As an example consider two counterpropagating laser beams that have orthogonal polarizations, as discussed below. The superposition of the two beams results in a light field having a polarization that varies on the wavelength scale along the direction of the laser beams. Laser cooling by such a light field is called polarization-gradient cooling. In a three-dimensional optical-molasses, the transverse wave character of light requires that the light field always has polarization gradients.

B. Linear ⊥ Linear Polarization Gradient Cooling

One of the most instructive models for discussion of sub-Doppler laser cooling was introduced in Ref. [20] and very well described in Ref. [18]. If the polarizations of two counterpropagating laser beams are identical, the two beams interfere and produce a standing-wave. When the two beams have orthogonal linear polarizations (same frequency ω_ℓ) with their $\hat{\varepsilon}$ vectors perpendicular (*e.g.*, $\hat{x}$ and $\hat{y}$), the configuration is called lin ⊥ lin or lin-perp-lin. Then the total field is the sum of the two counterpropagating beams given by

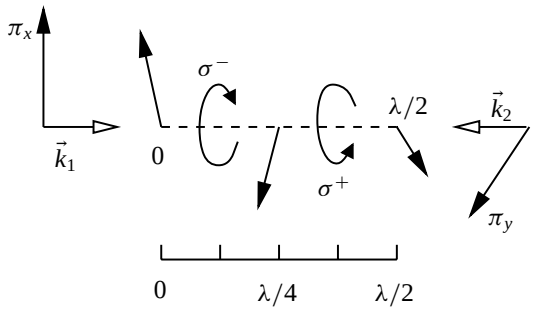

FIG. 7: Polarization gradient field for the lin ⊥ lin configuration.

$$\begin{aligned}\vec{E} &= E_0\,\hat{x}\,\cos(\omega_\ell t - kz) + E_0\,\hat{y}\,\cos(\omega_\ell t + kz) \qquad (27)\\ &= E_0\left[(\hat{x}+\hat{y})\cos\omega_\ell t\,\cos kz + (\hat{x}-\hat{y})\sin\omega_\ell t\,\sin kz\right].\end{aligned}$$

At the origin, where $z = 0$, this becomes

$$\vec{E} = E_0(\hat{x}+\hat{y})\cos\omega_\ell t, \qquad (28)$$

which corresponds to linearly polarized light at an angle $+\pi/4$ to the x-axis. The amplitude of this field is $\sqrt{2}E_0$. Similarly, for $z = \lambda/4$, where $kz = \pi/2$, the field is also linearly polarized but at an angle $-\pi/4$ to the x-axis.

Between these two points, at $z = \lambda/8$, where $kz = \pi/4$, the total field is

$$\vec{E} = E_0\left[\hat{x}\,\sin(\omega_\ell t + \pi/4) - \hat{y}\,\cos(\omega_\ell t + \pi/4)\right]. \qquad (29)$$

Since the $\hat{x}$ and $\hat{y}$ components have sine and cosine temporal dependence, they are $\pi/2$ out of phase, and so Eq. 29 represents circularly polarized light rotating about the z-axis in the negative sense. Similarly, at $z = 3\lambda/8$ where $kz = 3\pi/4$, the polarization is circular but in the positive sense. Thus in this lin ⊥ lin scheme the polarization cycles from linear to circular to orthogonal linear to opposite circular in the space of only half a wavelength of light, as shown in Fig. 7. It truly has a very strong polarization-gradient.

Since the coupling of the different states of multi-level atoms to the light field depends on its polarization, atoms moving in a polarization-gradient will be coupled differently at different positions, and this will have important consequences for laser cooling. For the $J_g = 1/2 \rightarrow J_e = 3/2$ transition (the simplest transition that shows sub-Doppler cooling), the optical pumping process in purely σ^+ light drives the ground-state population to the $M_g = +1/2$ sublevel. This optical-pumping occurs because absorption always produces $\Delta M = +1$ transitions, whereas the subsequent spontaneous emission produces $\Delta M = \pm 1, 0$. Thus the average $\Delta M \geq 0$ for each scattering event. For σ^--light the population is pumped toward the $M_g = -1/2$ sublevel. Thus atoms traveling through only a half wavelength in the light field, need to readjust their population completely from $M_g = +1/2$ to $M_g = -1/2$ and back again.

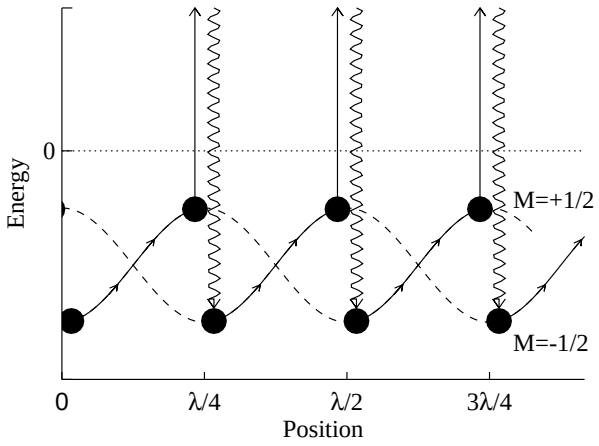

FIG. 8: The spatial dependence of the light shifts of the ground-state sublevels of the $J = 1/2 \Leftrightarrow 3/2$ transition for the case of the lin $\perp$ lin polarization configuration. The arrows show the path followed by atoms being cooled in this arrangement. Atoms starting at $z = 0$ in the $M_g = +1/2$ sublevel must climb the potential hill as they approach the $z = \lambda/4$ point where the light becomes σ^- polarized, and there they are optically pumped to the $M_g = -1/2$ sublevel. Then they must begin climbing another hill toward the $z = \lambda/2$ point where the light is σ^+ polarized and they are optically pumped back to the $M_g = +1/2$ sublevel. The process repeats until the atomic kinetic energy is too small to climb the next hill. Each optical pumping event results in absorption of light at a lower frequency than emission, thus dissipating energy to the radiation field.

The interaction between nearly resonant light and atoms not only drives transitions between atomic energy levels, but also shifts their energies. This light shift of the atomic energy levels plays a crucial role in this scheme of sub-Doppler cooling, and the changing polarization has a strong influence on the light shifts. In the low-intensity limit of two laser beams, each of intensity $s_0 I_s$, the light shifts ΔE_g of the ground magnetic substates are given by [1]

$$\Delta E_g = \frac{\hbar \delta s_0 C_{ge}^2}{1 + (2\delta/\gamma)^2}, \tag{30}$$

where C_{ge} is the Clebsch-Gordan coefficient that describes the coupling between the atom and the light field.

In the present case of orthogonal linear polarizations and $J = 1/2 \rightarrow 3/2$, the light shift for the magnetic substate $M_g = 1/2$ is three times larger than that of the $M_g = -1/2$ substate when the light field is completely σ^+. On the other hand, when an atom moves to a place where the light field is σ^-, the shift of $M_g = -1/2$ is three times larger. So in this case the optical-pumping discussed above causes there to be a larger population in the state with the larger light shift. This is generally true for any transition J_g to $J_e = J_g + 1$. A schematic diagram showing the populations and light shifts for this particular case of negative detuning is shown in Fig. 8.

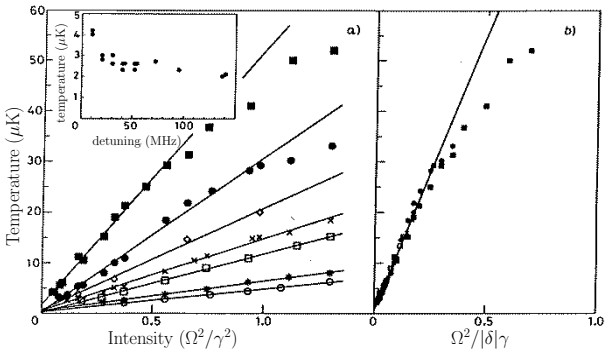

FIG. 9: Temperature as a function of laser intensity and detuning for Cs atoms in an optical molasses from Ref. [22]. a) Temperature as a function of the detuning for various intensities. b) Temperature as a function of the light shift. All the data points are on a universal straight line.

C. Origin of the Damping Force

To discuss the origin of the cooling process in this polarization gradient scheme, consider atoms with a velocity v at a position where the light is σ^+-polarized, as shown at the lower left of Fig. 8. The light optically pumps such atoms to the strongly negative light-shifted $M_g = +1/2$ state. In moving through the light field, atoms must increase their potential energy (climb a hill) because the polarization of the light is changing and the state $M_g = 1/2$ becomes less strongly coupled to the light field. After traveling a distance $\lambda/4$, atoms arrive at a position where the light field is σ^--polarized, and are optically pumped to $M_g = -1/2$, which is now lower than the $M_g = 1/2$ state. Again the moving atoms are at the bottom of a hill and start to climb. In climbing the hills, the kinetic energy is converted to potential energy, and in the optical-pumping process, the potential energy is radiated away because the spontaneous-emission is at a higher frequency than the absorption (see Fig. 8). Thus atoms seem to be always climbing hills and losing energy in the process. This process brings to mind a Greek myth, and is thus called "Sisyphuslaser-cooling".

The cooling process described above is effective over a limited range of atomic velocities. The force is maximum for atoms that undergo one optical-pumping process while traveling over a distance $\lambda/4$. Slower atoms will not reach the hilltop before the pumping process occurs and faster atoms will already be descending the hill before being pumped toward the other sublevel. In both cases the energy loss is smaller and therefore the cooling process less efficient. Nevertheless, the damping constant β for this process is much larger than for Doppler cooling, and therefore the final steady-state temperature is lower [18, 20].

In the experiments of Ref. [22], the temperature was measured in a 3D molasses under various configurations of the polarization. Temperatures were measured by a

ballistic technique, where the flight time of the released atoms was measured as they fell through a probe a few cm below the molasses region. Results of their measurements are shown in Fig. 9a, where the measured temperature is plotted for different detunings as a function of the intensity. For each detuning, the data lie on a straight line through the origin. The lowest temperature obtained is 3 μK, which is a factor 40 below the Doppler temperature and a factor 15 above the recoil-temperature of Cs. If the temperature is plotted as a function of the light-shift (see Fig. 9b), all the data are on a single universal straight line.

D. The Limits of Laser Cooling

The lower limit to Dopplerłaser-cooling of two-level atoms arises from the competition with heating. This cooling limit is described as a random walk in momentum space whose steps are of size $\hbar k$ and whose rate is the scattering rate, $\gamma_p = s_0\gamma/2$ for zero detuning and $s_0 \ll 1$. As long as the force can be accurately described as a damping force, then the Fokker-Planck-equation is applicable, and the outcome is a lower limit to the temperature of laser cooling given by the Doppler temperature $k_B T_D \equiv \hbar\gamma/2$.

The extension of this kind of thinking to the sub-Doppler processes described in Sec. VI B must be done with some care, because a naive application of the consequences of the Fokker-Planck-equation would lead to an arbitrarily low final temperature. In the derivation of the Fokker-Planck-equation it is explicitly assumed that each scattering event changes the atomic momentum p by an amount that is a small fraction of p as embodied in Eq. **??**, and this clearly fails when the velocity is reduced to the region of $v_r \equiv \hbar k/M$.

This limitation of the minimum steady-state value of the average kinetic energy to a few times $2E_r \equiv k_B T_r = Mv_r^2$ is intuitively comforting for two reasons. First, one might expect that the last spontaneous-emission in a cooling process would leave atoms with a residual momentum of the order of $\hbar k$, since there is no control over its direction. Thus the randomness associated with this would put a lower limit on such cooling of $v_{\min} \sim v_r$. Second, the polarization-gradient-cooling mechanism described above requires that atoms be localizable within the scale of $\sim \lambda/2\pi$ in order to be subject to only a single polarization in the spatially inhomogeneous light field. The uncertainty-principle then requires that these atoms have a momentum spread of at least $\hbar k$.

The recoil limit discussed here has been surpassed by evaporative cooling of trapped atoms [23] and two different optical cooling methods, neither of which can be based in simple notions. One of these uses optical pumping into a velocity-selective dark state and is described in Ref. [1] The other one uses carefully chosen, counterpropagating laser pulses to induce velocity-selective Raman transitions, and is called Raman-cooling [24].

VII. TRAPPING OF NEUTRAL ATOMS

A. Introduction

Although ion trapping, laser cooling of trapped ions, and trapped ion spectroscopy were known for many years [25], it was only in 1985 that neutral atoms were first trapped [26]. Confinement of neutral atoms depends on the interaction between an inhomogeneous electromagnetic field and an atomic multipole moment. Unperturbed atoms do not have electric dipole moments because of their inversion symmetry, and therefore electric (*e.g.*, optical) traps require induced dipole moments. This is often done with nearly resonant optical fields, thus producing the optical traps discussed below. On the other hand, many atoms have ground- or metastable-state magnetic dipole moments that may be used for trapping them magnetically.

In order to confine any object, it is necessary to exchange kinetic for potential energy in the trapping field, and in neutral atom traps, the potential energy must be stored as internal atomic energy. There are two immediate and extremely important consequences of this requirement. First, the atomic energy levels will necessarily shift as the atoms move in the trap, and these shifts will affect the precision of spectroscopic measurements, perhaps severely. Second, practical traps for ground-state neutral atoms are necessarily very shallow compared with thermal energy because the energy level shifts that result from convenient size fields are typically considerably smaller than $k_B T$ for $T = 1$ K. Neutral atom trapping therefore depends on substantial cooling of a thermal atomic sample, and is often connected with the cooling process.

The small depth of neutral atom traps also dictates stringent vacuum requirements, because an atom cannot remain trapped after a collision with a thermal energy background gas molecule. Since these atoms are vulnerable targets for thermal energy background gas, the mean free time between collisions *must* exceed the desired trapping-time. The cross section for destructive collisions is quite large because even a gentle collision (*i.e.*, large impact parameter) can impart enough energy to eject an atom from a trap. At pressure P sufficiently low to be of practical interest, the trapping time is $\sim (10^{-8}/P)$ s, where P is in Torr.

B. Magnetic Traps

An atom with a magnetic moment $\vec{\mu}$ can be confined by an inhomogeneous magnetic field because of an interaction between the moment and the field. This produces a force given by $\vec{F} = \vec{\nabla}(\vec{\mu} \cdot \vec{B})$. Several different magnetic traps with varying geometries that exploit this force have been studied in some detail, and their general features have been presented [27]. The simplest magnetic trap is a quadrupole comprised of two identical coils carrying opposite currents (see Fig. 10) that has a single center where the field is zero. When the coils are separated by 1.25 times their radius, such a trap has equal depth in the radial (x-y plane) and longitudinal (z-axis) directions [27]. Its experimental simplicity makes it most attractive, both because of ease of construction and of optical access to the interior. Such a trap was used in the first neutral atom trapping experiments at NIST.

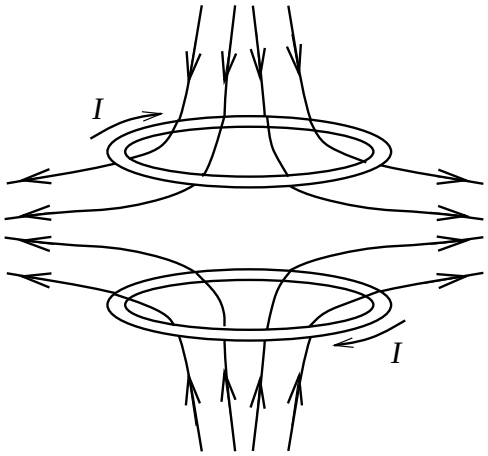

FIG. 10: Schematic diagram of the coil configuration used in the quadrupole trap and the resultant magnetic field lines. Because the currents in the two coils are in opposite directions, there is a $|\vec{B}| = 0$ point at the center.

The magnitude of the field is zero at the center of this trap, and increases in all directions as $B = A\sqrt{\rho^2 + 4z^2}$, where $\rho^2 \equiv x^2 + y^2$, and the field gradient A is constant. The field gradient is fixed along any line through the origin, but has different values in different polar directions. Therefore the force that confines the atoms in the trap is neither harmonic nor central, and angular-momentum is not conserved. There are several motivations for studying the motion of atoms in a magnetic trap. Knowing their positions may be important for trapped atom spectroscopy. Moreover, simply studying the motion for its own sake has turned out to be an interesting problem because the distorted conical potential of the quadrupole trap does not have analytic solutions, and its bound states are not well known. For the two-coil quadrupole magnetic trap of Fig. 10, stable circular orbits can be found classically [1]. The fastest trappable atoms in circular orbits have $v_{\max} \sim 1$ m/s so the orbital frequency becomes $\omega_T/2\pi \sim 20$ Hz. Because of the anharmonicity of the potential, the orbital frequencies depend on the orbit size, but in general, atoms in lower energy orbits have higher frequencies.

Because of the dependence of the trapping force on the angle between the field and the atomic moment the orientation of the magnetic moment with respect to the field must be preserved as the atoms move about in the trap. This requires velocities low enough to ensure that the interaction between the atomic moment $\vec{\mu}$ and the field

$\vec{B}$ is adiabatic, especially when the atom's path passes through a region where the field magnitude is small. This is especially critical at the low temperatures of the Bose condensation experiments. Therefore energy considerations that focus only on the trap depth are not sufficient to determine the stability of a neutral atom trap: orbit and/or quantum state calculations and their consequences must also be considered.

The condition for adiabatic motion can be written as $\omega_Z \gg |\mathrm{d}B/\mathrm{d}t|/B$, where $\omega_Z = \mu B/\hbar$ is the Larmor precession rate in the field. The orbital frequency for circular motion is $\omega_T = v/\rho$, and since $v/\rho = |\mathrm{d}B/\mathrm{d}t|/B$ for a uniform field gradient, the adiabaticity condition is $\omega_Z \gg \omega_T$. For the two-coil quadrupole trap, the adiabaticity condition can be easily calculated [1]. A practical trap ($A \sim 1$ T/m) requires $\rho \gg 1$ μm as well as $v \gg 1$ cm/s. Note that violation of these conditions results in the onset of quantum dynamics for the motion (deBroglie wavelength $\approx$ orbit size). Since the non-adiabatic region of the trap is so small (less than 10^{-18} m^3 compared with typical sizes of ~ 2 cm corresponding to 10^{-5} m^3), nearly all the orbits of most atoms are restricted to regions where they are adiabatic.

Modern techniques of laser and evaporative cooling have the capability to cool atoms to energies where their deBroglie wavelengths are on the micron scale. Such cold atoms may be readily confined to micron size regions in magnetic traps with easily achievable field gradients, and in such cases, the notion of classical orbits is inappropriate. The motional dynamics must be described in terms of quantum mechanical variables and suitable wavefunctions. Furthermore, the distribution of atoms confined in various quantum states of motion in quadrupole as well as other magnetic traps is critical for interpreting the measurements on Bose condensates.

Studying the behavior of extremely slow (cold) atoms in the two-coil quadrupole trap begins with a heuristic quantization of the orbital angular momentum using $Mr^2\omega_T = n\hbar$ for circular orbits [1]. For velocities of optically cooled atoms of a few cm/s, $n \sim$ 10–100. By contrast, evaporative-cooling [23] can produce velocities ~ 1 mm/s resulting in $n \sim 1$. It is readily found that $\omega_Z = n\omega_T$, so that the adiabatic condition is satisfied only for $n \gg 1$. The separation of the rapid precession from the slower orbital motion is reminiscent of the Born-Oppenheimer approximation for molecules, and three dimensional quantum calculations have also been described [1].

C. Optical Traps

Optical trapping of neutral atoms by electrical interaction must proceed by inducing a dipole moment. For dipole optical traps, the oscillating electric field of a laser induces an oscillating atomic electric dipole moment that interacts with the laser field. If the laser field is spatially inhomogeneous, the interaction and associated energy level shift of the atoms varies in space and therefore produces a potential. When the laser frequency is tuned below atomic resonance ($\delta < 0$), the sign of the interaction is such that atoms are attracted to the maximum of laser field intensity, whereas if $\delta > 0$, the attraction is to the minimum of field intensity.

The simplest imaginable trap consists of a single, strongly focused Gaussianłaser-beam [28, 29] whose intensity at the focus varies transversely with r as $I(r) = I_0 e^{-r^2/w_0^2}$, where w_0 is the beam waist size. Such a trap has a well-studied and important macroscopic classical analog in a phenomenon called optical tweezers [30–32]. With the laser light tuned below resonance ($\delta < 0$), the ground-state light shift is everywhere negative, but largest at the center of the Gaussian beam waist. Ground-state atoms therefore experience a force attracting them toward this center given by the gradient of the light-shift. In the longitudinal direction there is also an attractive force that depends on the details of the focusing. Thus this trap produces an attractive force on atoms in three dimensions.

The first optical trap was demonstrated in Na with light detuned below the D-lines [29]. With 220 mW of dye laser light tuned about 650 GHz below the Na transition and focused to a ~ 10 μm waist, the trap depth was about $15\hbar\gamma$ corresponding to 7 mK. Single-beam dipole force traps can be made with the light detuned by a significant fraction of its frequency from the atomic transition. Such a far-off-resonance trap (FORT) has been developed for Rb atoms using light detuned by nearly 10% to the red of the D_1 transition at $\lambda = 795$ nm [33]. Between 0.5 and 1 W of power was focused to a spot about 10 μm in size, resulting in a trap 6 mK deep where the light scattering rate was only a few hundred/s. The trap lifetime was more than half a second.

The dipole force for blue light repels atoms from the high intensity region, and offers the advantage that trapped atoms will be confined where the perturbations of the light field are minimized [1]. On the other hand, it is not as easy to produce hollow light beams compared with Gaussian beams, and special optical techniques need to be employed.

In a standing-wave the light intensity varies from zero at a node to a maximum at an antinode in a distance of $\lambda/4$. Since the light-shift, and thus the optical-potential, vary on this same scale, it is possible to confine atoms in wavelength-size regions of space. Of course, such tiny traps are usually very shallow, so loading them requires cooling to the μK regime. The momentum of such cold atoms is then so small that their deBroglie wavelengths are comparable to the optical wavelength, and hence to the trap size. In fact, the deBroglie wavelength equals the size of the optical traps ($\lambda/2$) when the momentum is $2\hbar$k, corresponding to a kinetic energy of a few μK. Thus the atomic motion in the trapping volume is not classical, but must be described quantum mechanically. Even atoms whose energy exceeds the trap depth must be described as quantum mechanical particles moving in a pe-

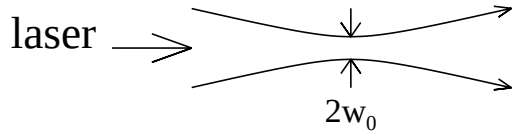

FIG. 11: A single focused laser beam produces the simplest type of optical trap.

riodic potential that display energy-band structure [34].

Atoms trapped in wavelength-sized spaces occupy vibrationalłevels similar to those of molecules. The optical spectrum can show Raman-like sidebands that result from transitions among the quantized vibrational levels [35, 36] as shown in Fig. 19. These quantum states of atomic motion can also be observed by spontaneous or stimulated emission [35, 37]. Considerably more detail about atoms in such optical lattices is to be found in Ref. [36].

D. Magneto-Optical Traps

The most widely used trap for neutral atoms is a hybrid, employing both optical and magnetic fields, to make a magneto-optical trap (MOT) first demonstrated in 1987 [38]. The operation of a MOT depends on both inhomogeneous magnetic fields and radiative selection rules to exploit both optical pumping and the strong radiative force [1, 38]. The radiative interaction provides cooling that helps in loading the trap, and enables very easy operation. The MOT is a very robust trap that does not depend on precise balancing of the counterpropagating laser beams or on a very high degree of polarization. The magnetic field gradients are modest and can readily be achieved with simple, air-cooled coils. The trap is easy to construct because it can be operated with a room-temperature cell where alkali atoms are captured from the vapor. Furthermore, low-cost diode lasers can be used to produce the light appropriate for all the alkalis except Na, so the MOT has become one of the least expensive ways to produce atomic samples with temperatures below 1 mK. For these and other reasons it has become the workhorse of cold atom physics, and has also appeared in dozens of undergraduate laboratories.

Trapping in a MOT works by optical pumping of slowly moving atoms in a linearly inhomogeneous magnetic field $B = B(z) \equiv Az$, such as that formed by a magnetic quadrupole-field. Atomic transitions with the simple scheme of $J_g = 0 \rightarrow J_e = 1$ have three Zeeman components in a magnetic field, excited by each of three polarizations, whose frequencies tune with field (and therefore with position) as shown in Fig. 12 for 1D. Two counterpropagating laser beams of opposite circular polarization, each detuned below the zero field atomic resonance by δ, are incident as shown.

Because of the Zeeman shift, the excited state $M_e = +1$ is shifted up for $B > 0$, whereas the state with $M_e = -1$ is shifted down. At position z' in Fig. 12 the magnetic field therefore tunes the $\Delta M = -1$ transition closer to resonance and the $\Delta M = +1$ transition further out of resonance. If the polarization of the laser beam incident from the right is chosen to be σ^- and correspondingly σ^+ for the other beam, then more light is scattered from the σ^- beam than from the σ^+ beam. Thus the atoms are driven toward the center of the trap where the magnetic field is zero. On the other side of the center of the trap, the roles of the $M_e = \pm 1$ states are reversed and now more light is scattered from the σ^+ beam, again driving the atoms towards the center.

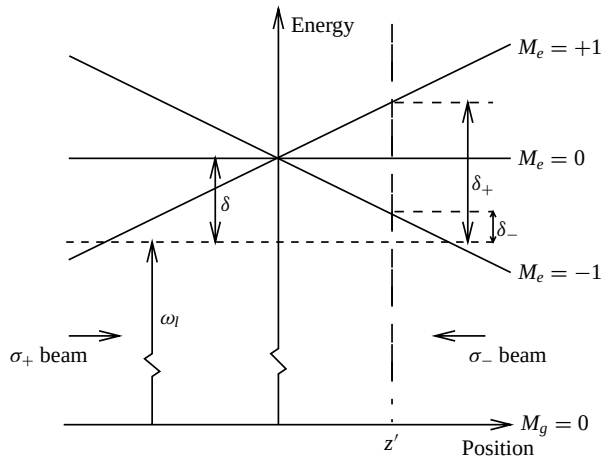

FIG. 12: Arrangement for a MOT in 1D. The horizontal dashed line represents the laser frequency seen by an atom at rest in the center of the trap. Because of the Zeeman shifts of the atomic transition frequencies in the inhomogeneous magnetic field, atoms at $z = z'$ are closer to resonance with the σ^- laser beam than with the σ^+ beam, and are therefore driven toward the center of the trap.

The situation is analogous to the velocity damping in an optical molasses from the Doppler effect as discussed above, but here the effect operates in position space, whereas for molasses it operates in velocity space. Since the laser light is detuned below the atomic resonance in both cases, compression and cooling of the atoms is obtained simultaneously in a MOT.

For a description of the motion of the atoms in a MOT, consider the radiative force in the low intensity limit (see Eq. 10). The total force on the atoms is given by $\vec{F} = \vec{F}_+ + \vec{F}_-$, where

$$\vec{F}_\pm = \pm \frac{\hbar \vec{k} \gamma}{2} \frac{s_0}{1 + s_0 + (2\delta_\pm/\gamma)^2} \tag{31}$$

and the detuning $\delta_\pm$ for each laser beam is given by

$$\delta_\pm = \delta \mp \vec{k} \cdot \vec{v} \pm \mu' B/\hbar. \tag{32}$$

Here $\mu' \equiv (g_e M_e - g_g M_g)\mu_B$ is the effective magnetic moment for the transition used. Note that the Doppler

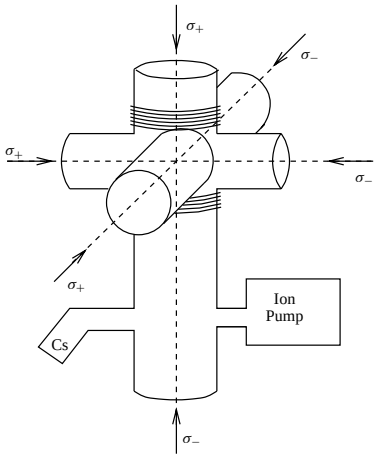

FIG. 13: The schematic diagram of a MOT shows the coils and the directions of polarization of the six light beams. It has an axial symmetry and various rotational symmetries, so some exchanges would still result in a trap that works, but not all configurations are possible. Atoms are trapped from the background vapor of Cs that arises from a piece of solid Cs in one of the arms of the setup.

shift $\omega_D \equiv -\vec{k}\cdot\vec{v}$ and the Zeeman shift $\omega_Z = \mu' B/\hbar$ both have opposite signs for opposite beams.

When both the Doppler and Zeeman shifts are small compared to the detuning δ, the denominator of the force can be expanded and the result becomes $\vec{F} = -\beta\vec{v} - \kappa\vec{r}$, where β is the damping coefficient. The spring constant κ arises from the similar dependence of $\vec{F}$ on the Doppler and Zeeman shifts, and is given by $\kappa = \mu' A\beta/\hbar k$. This force leads to damped harmonic motion of the atoms, where the damping rate is given by $\Gamma_{\rm MOT} = \beta/M$ and the oscillation frequency $\omega_{\rm MOT} = \sqrt{\kappa/M}$. For magnetic field gradients $A \approx 10$ G/cm, the oscillation frequency is typically a few kHz, and this is much smaller than the damping rate that is typically a few hundred kHz. Thus the motion is overdamped, with a characteristic restoring time to the center of the trap of $2\Gamma_{\rm MOT}/\omega^2_{\rm MOT} \sim$ several ms for typical values of the detuning and intensity of the lasers.

Since the MOT constants β and κ are proportional, the size of the atomic cloud can easily be deduced from the temperature of the sample. The equipartition of the energy of the system over the degrees of freedom requires that the velocity spread and the position spread are related by $k_B T = m v^2_{\rm rms} = \kappa z^2_{\rm rms}$. For a temperature in the range of the Doppler temperature, the size of the MOT should be of the order of a few tenths of a mm, which is generally the case in experiments.

So far the discussion has been limited to the motion of atoms in 1D. However, the MOT scheme can easily be extended to 3D by using six instead of two laser beams. Furthermore, even though very few atomic species have transitions as simple as $J_g = 0 \rightarrow J_e = 1$, the scheme works for any $J_g \rightarrow J_e = J_g + 1$ transition. Atoms that scatter mainly from the σ^+ laser beam will be optically pumped toward the $M_g = +J_g$ substate, which forms a closed system with the $M_e = +J_e$ substate.

The atomic density in a MOT cannot increase without limit as more atoms are added. The density is limited to $\sim 10^{11}/{\rm cm}^3$ because the fluorescent light emitted by some trapped atoms is absorbed by others, and this diffusion of radiation presents a repulsive force between the atoms [39, 40]. Another limitation lies in the collisions between the atoms, and the collision rate for excited atoms is much larger than for ground-state atoms. Adding atoms to a MOT thus increases the density up to some point, but adding more atoms then expands the volume of the trapped sample.

VIII. APPLICATIONS

A. Introduction

The techniques of laser cooling and trapping as described in the previous sections have been used to manipulate the positions and velocities of atoms with unprecedented variety and precision [1]. These techniques are currently used in the laboratories to design new, highly sensitive experiments that move experimental atomic physics research to completely new regimes. In this section only of few of these topics will be discussed. One of the most straightforward of these is the use of laser cooling to increase the brightness of atomic beams which can subsequently be used for different types of experiments. Since laser cooling produces atoms at very low temperatures, the interaction between these atoms also takes place at such very low energies. The study of these interactions, called ultra-cold collisions, has been a very fruitful area of research in the last decade.

The atom-laser interaction not only produces a viscous environment for cooling the atoms down to very low velocities, but also provides a trapping field for the atoms. In the case of interfering laser beams, the size of such traps can be of the order of a wavelength, thus providing microscopic atomic traps with a periodic structure. These optical lattices described in section VIII E below provide a versatile playground to study the effects of a periodic potential on the motion of atoms and thus simulate the physics of condensed matter. Another topic of considerable interest discussed below in section VIII F exists only because laser cooling has paved the way to the observation of Bose-Einstein condensation. This was predicted theoretically more than 80 years ago, but was observed in a dilute gas for the first time in 1996. Finally, the physics of dark states is discussed in section VIII G. These show a rich variety of effects caused by the coupling of internal and external coordinates of atoms.

B. Atomic Beam Brightening

In considering the utility of atomic beams for the purposes of lithography, collision studies, or a host of other applications, maximizing the beam intensity may not be the best option. Laser cooling can be used for increasing the phase space density and this notion applies to both atomic traps and atomic beams. In the case of atomic beams, other quantities than phase space density have been defined as well, but these are not always consistently used. The geometrical solid angle occupied by atoms in a beam is $\Delta\Omega = (\Delta v_\perp/\bar{v})^2$, where $\bar{v}$ is some measure of the average velocity of atoms in the beam and $\Delta v_\perp$ is a measure of the width of the transverse velocity distribution of the atoms. The total current or flux of the beam is Φ, and the flux density or intensity is $\Phi/\pi(\Delta x)^2$ where Δx is a measure of the beam's radius. Then the beam brightness or radiance R is given by $R = \Phi/\pi(\Delta x_\perp)^2\Delta\Omega$.

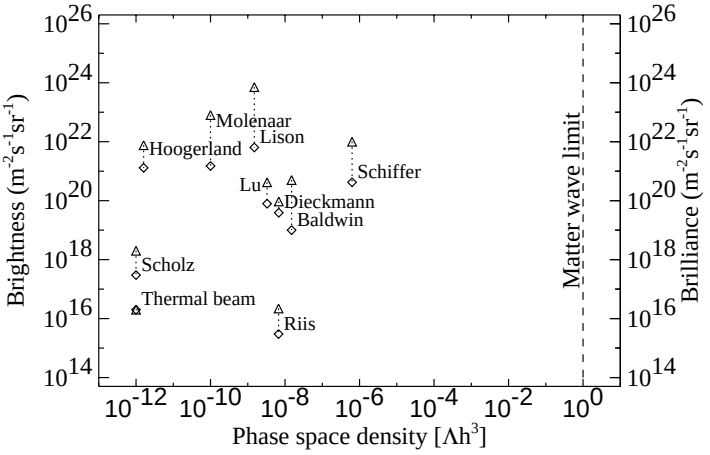

FIG. 14: Plot of brightness (diamonds) and brilliance (triangles) *vs.* phase space density for various atomic beams cited in the literature. The lower-left point is for a normal thermal beam, and the progression toward the top and right has been steady since the advent of laser cooling. The experimental results are from Riis *et al.* [41], Scholz *et al.* [42], Hoogerland *et al.* [43], Lu *et al.* [44], Baldwin *et al.* [45], Molenaar *et al.* [10], Schiffer *et al.* [46], Lison *et al.* [47] and Dieckmann *et al.* [48]. The quantum boundary for Bose-Einstein condensation (see section VIII F), where the phase space density is unity, is shown by the dashed line of the right (figure adapted from Ref. [47]).

Optical beams are often characterized by their frequency spread, and, because of the deBroglie relation $\lambda = h/p$, the appropriate analogy for atomic beams is the longitudinal velocity spread. Thus the spectral-brightness or brilliance B, is given by $B = R\bar{v}/\Delta v_z$. Note that both R and B have the same dimensions as flux density, and this is often a source of confusion. Finally, B is simply related to the 6D phase space density. Recently a summary of these beam properties has been presented in the context of phase space (see Fig. 14).

One of the first beam-brightening experiments was performed by Nellesen *et al.* [49, 50] where a thermal beam of Na was slowed with the chirp technique [1]. Then the slow atoms were deflected out of the main atomic beam and transversely cooled. In a later experiment [51] this beam was fed into a two-dimensional MOT where the atoms were cooled and compressed in the transverse direction by an optical molasses of σ^+-σ^- polarized light. Another approach was used by Riis *et al.* who directed a slowed atomic beam into a hairpin-shaped coil that they called an "atomic funnel" [41]. The wires of this coil generated a two-dimensional quadrupole field that was used as a two-dimensional MOT as described before.

These approaches yield intense beams when the number of atoms in the uncooled beam is already high. However, if the density in the beam is initially low, for example in the case of metastable noble gases or radioactive isotopes, one has to capture more atoms from the source in order to obtain an intense beam. Aspect *et*

al. [52] have used a quasi-standing wave of converging laser beams whose incidence angle varied from 87° to 90° to the atomic beam direction, so that a larger solid angle of the source could be captured. In this case they used a few mW of laser light over a distance of 75 mm. One of the most sophisticated approaches to this problem has been developed for metastable Ne by Hoogerland *et al.* [43]. They used a three-stage process to provide a large solid angle capture range and produce a high brightness beam.

C. Applications to Atomic Clocks

Perhaps one of the most important practical applications of laser cooling is the improvement of atomic clocks. The limitation to both the accuracy and precision of such clocks is imposed by the thermal motion of the atoms, so a sample of laser-cooled atoms could provide a substantial improvement in clocks and in spectroscopic resolution.

The first experiments intended to provide slower atoms for better precision or clocks were attemps at an atomic fountain by Zacharias in the 1950's [1, 53]. This failed because collisions depleted the slow atom population, but the advent of laser cooling enabled an atomic fountain because the slow atoms far outnumber the faster ones. The first rf spectroscopy experiments in such a fountain using laser cooled atoms were reported in 1989 and 1991 [54, 55], and soon after that some other laboratories also reported successes.

Some of the early best results were reported by Gibble and Chu [56, 57]. They used a MOT with laser beams 6 cm in diameter to capture Cs atoms from a vapor at room temperature. These atoms were launched upward at 2.5 m/s by varying the frequencies of the MOT lasers to form a moving optical molasses as described in section V, and subsequently cooled to below 3 μK. The atoms were optically pumped into one hfs sublevel, then passed through a 9.2 GHz microwave-cavity on their way up and again later on their way down. The number of atoms that were driven to change their hfs state by the microwaves was measured *vs.* microwave frequency, and the signal showed the familiar Ramsey oscillations (see chapter "Coherent Optical Transients" for a discussion of Ramsey fringes). The width of the central feature was 1.4 Hz and the S/N was over 50. Thus the ultimate precision was 1.5 mHz corresponding to $\delta\nu/\nu \cong 10^{-12}/\tau^{1/2}$ where τ is the number of seconds for averaging.

The ultimate limitation to the accuracy of this experiment as an atomic clock was collisions between Cs atoms in the beam. Because of the extremely low relative velocities of the atoms, the cross sections are very large (see section VIII D below) and there is a measurable frequency shift [58]. By varying the density of Cs atoms in the fountain, the authors found frequency shifts of the order of a few mHz for atomic density of $10^9/\text{cm}^3$, depending on the magnetic sublevels connected by the microwaves. Extrapolation of the data to zero density provided a frequency determination of $\delta\nu/\nu \cong 4\times10^{-14}$. More recently the frequency shift has been used to determine a scattering-length of -400a_0 [59] so that the expected frequency shift is 10^4 times larger than other limitations to the clock at an atomic density of n=$10^9/\text{cm}^3$. Thus the authors suggest possible improvements to atomic time keeping of a factor of 1000 in the near future. Even more promising are cold atom clocks in orbit (microgravity) where the interaction time can be very much longer than 1 s [60].

D. Ultra-cold Collisions

Laser-cooling techniques were developed in the early 1980s for a variety of reasons, such as high-resolution spectroscopy [1]. During the development of the techniques to cool and trap atoms, it became apparent that collisions between cold atoms in optical traps was one of the limiting factors in the achievement of high density samples. Trap loss experiments revealed that the main loss mechanisms were caused by laser-induced collisions. Further cooling and compression could only be achieved by techniques not exploiting laser light, such as evaporative cooling in magnetic traps. Elastic collisions between atoms in the ground state are essential in that case for the rethermalization of the sample, whereas inelastic collisions lead to destruction of the sample. Knowledge about collision physics at these low energies is therefore essential for the development of high-density samples of atoms using either laser or evaporative cooling techniques.

Ground-state collisions play an important role in evaporative cooling. Such elastic collisions are necessary to obtain a thermalization of the gas after the trap depth has been lowered, and a large elastic cross section is essential to obtain a rapid thermalization. Inelastic collisions, on the other hand, can release enough energy to accelerate the atoms to energies too high to remain trapped. Ground-state collisions for evaporative cooling can be described by one parameter, the scattering-length a. At temperatures below T_D, these collisions are in the s-wave scattering regime where only the phase-shift δ_0 of the lowest partial wave $\ell = 0$ is important. Moreover, for sufficiently low energies, such collisions are governed by the Wigner threshold laws where the phase shift δ_0 is inversely proportional to the wavevector k of the particle motion. Taking the limit for low energy gives the proportionality constant, defined as the scattering length $a = -\lim_{k\to0}(\delta_0/k)$. The scattering length not only plays an important role in ultra-cold collisions, but also in the formation of Bose-Einstein condensates (see section VIII F). In the Wigner-threshold regime the cross-section approaches a constant, $\sigma = 8\pi a^2$ [61].

Although ground-state collisions are important for evaporative cooling and BEC, they do *not* provide a very versatile research field from a collision physics point of view. The situation is completely different for the excited-state collisions. For typical temperatures in opti-

cal traps, the velocity of the atoms is sufficiently low that atoms excited at long range by laser light decay before the collision takes place. Laser excitation for low-energy collisions has to take place during the collision. By tuning the laser frequency, the collision dynamics can be altered and information on the states formed in the molecular system can be obtained. This is the basis of the new technique of photo-associative spectroscopy, which for the first time has identified purely long-range states in diatomic molecules [1, 62].

For atoms colliding in laser light closely tuned to the S-P transition, the potential is a C_3/R^3 dipole-dipole interaction when one of the atoms is excited. Absorption takes place at the Condon point R_C given by $\hbar\delta = -C_3/R_C^3$ or $R_C = (C_3/\hbar|\delta|)^{1/3}$. Note that the light has to be tuned below resonance, which is mostly the case for laser cooling. The Condon-point for laser light detuned a few γ below resonance is typical 1000–2000 a_0.

Once the molecular complex becomes excited, it can evolve to smaller internuclear distances before emission takes place. Two particular cases are important for trap loss: (1) The emission of the molecular complex takes place at much smaller internuclear distance, and the energy gained between absorption and emission of the photon is converted into kinetic energy, or (2) The complex undergoes a transition to another state and the potential energy difference between the two states is converted into kinetic energy. In both cases the energy gain can be sufficient to eject one or both atoms out of the trap. In the case of the alkalis, the second reaction can take place because of the different fine-structure states and the reaction is denoted as a fine-structure changing collision. The first reaction is referred to as radiative-escape.

Trap loss collisions in MOT's have been studied to great extent, but results of these studies have to be considered with care. In most cases, trap loss is studied by changing either the frequency or the intensity of the trapping laser, which also changes the conditions of the trap. The collision rate is not only changed because of a change in the collision cross section, but also because of changes in both the density and temperature of the atoms in the trap. Since these parameters cannot be determined with high accuracy in a high-density trap, where effects like radiation trapping can play an important role, obtaining accurate results this way is very difficult.

The first description of such processes was given by Gallagher and Pritchard [63]. In their semiclassical model (the GP-model), the laser light is assumed to be weak enough that the excitation rate can be described by a quasi-static excitation probability. Atoms in the excited state are accelerated toward one another by the C_3/R^3 potential. In order to calculate the survival of the atoms in the excited state, the elapsed time between excitation and arrival is calculated. The total number of collisions is then given by the number of atoms at a certain distance, the fraction of atoms in the excited state, and the survival rate, integrated over all distances. For small detunings, corresponding to large internuclear distances, the excitation rate is appreciable over a very large range of internuclear distances. However the excitation occurs at large internuclear distances so the survival rate of the excited atoms is small. For large detunings the excitation is located in a small region at small internuclear distances, so the total excitation rate is small, but the survival rate is large. As a result of this competition, the collision rate peaks at intermediate detunings.

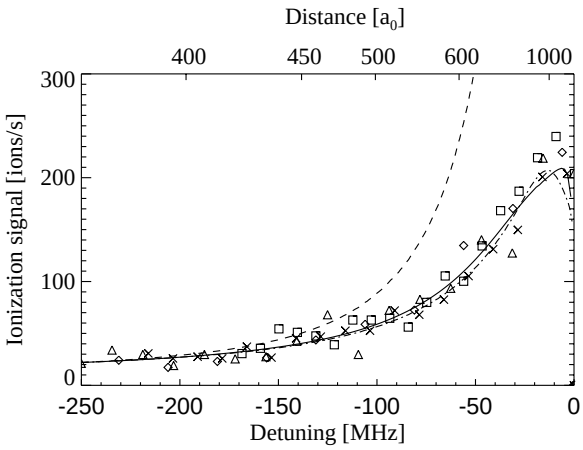

FIG. 15: The frequency dependence for the associative ionization rate of cold He* collisions. The experimental results (symbols) is compared with the semiclassical model (solid line), JV-model (dashed line), and modified JV-model (dashed-dotted line). The axis on top of the plot shows the Condon point, where the excitation takes place.

Another description of optical collisions is given by Julienne and Vigue [64]. Their description of optical collisions (JV-model) is quantum mechanical for the collision process, where they make a partial wave expansion of the incoming wavefunction. The authors describe the excitation process in the same way as it was done in the GP-model. Thus the excitation is localized around the Condon-point with a probability given by the quasi-static Lorentz formula.

In still another approach, a completely semiclassical description of optical collisions has been given by Mastwijk *et al.* [65]. These authors start from the GP-model, but make several important modifications. First, the Lorentz formula is replaced by the Landau-Zener formula. Second, the authors consider the motion of the atoms in the collision plane. At the Condon point, where the excitation takes place, the trajectory of the atom in the excited state is calculated by integration of the equation of motion. The results for their model are shown in Fig 15, and are compared with experiment and the JV-model. The agreement between the theory and experiment is rather good. For the JV-model two curves are shown. The first curve shows the situation for the original JV-model. The second curve shows the result of a modified JV-model, where the quasi-static excitation rate is replaced by the Landau-Zener formula. The large discrepancies between the results for these two models

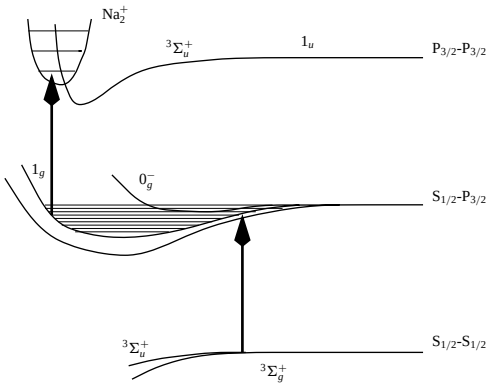

FIG. 16: Photoassociation spectroscopy of Na. By tuning the laser below atomic resonance, molecular systems can be excited to the first excited state, in which they are bound. By absorption of a second photon the system can be ionized, providing a high detection efficiency.

indicates that it is important to use the correct model for the excitation. The agreement between the modified JV-model and the semiclassical model is good, indicating that the dynamics of optical collisions can be described correctly quantum mechanically or semiclassically. Since the number of partial waves in the case of He* is in the order of 10, this is to be expected.

The description of optical collisions above applies to the situation that the quasi-molecule can be excited for each frequency of the laser light. However, the quasi-molecule has well-defined vibrational and rotational states and the excitation frequency has to match the transition frequency between the ground and excited rovibrational states. Far from the dissociation limit, the rovibrational states are well-resolved and many resonances are observed. This has been the basis of the method of photo-associative spectroscopy (PAS) for alkali-metal-atoms, where detailed information on molecular states of alkali dimers have been obtained recently. Here photo-association refers to the process where a photon is absorbed to transfer the system from the ground to the excited state where the two atoms are bound by their mutual attraction.

The process of PAS is depicted graphically in Fig. 16. When two atoms collide in the ground state, they can be excited at a certain internuclear distance to the excited molecular state and the two atoms may remain bound after the excitation and form a molecule. This transient molecule lives as long as the systems remains excited. The number of rotational states that can contribute to the spectrum is small for low temperature. The resolution is limited only by the linewidth of the transition, which is comparable to the natural linewidth of the atomic transition. With PAS, molecular states can be detected with a resolution of $\approx$10 MHz, which is many orders of magnitude better than traditional molecular spectroscopy. The formation of the molecules is probed by absorption of a second photon of the same color, which can ionize the molecule.

PAS has also been discussed in the literature as a technique to produce cold molecules. The methods discussed employ a double resonance technique, where the first color is used to create a well-defined rovibrational state of the molecule and a second color causes stimulated emission of the system to a well-defined vibrational level in the ground state. Although such a technique has not yet been shown to work experimentally, cold-molecules have been produced in PAS recently using a simpler method [66]. The 0_g^- state in Cs_2 has a double-well structure, where the top of the barrier is accidentally close to the asymptotic limit. Thus atoms created in the outer well by PAS can tunnel through the barrier to the inner well, where there is a large overlap of the wavefunction with the vibrational levels in the ground state. These molecules are then stabilized against spontaneous decay and can be observed. The temperature of the cold molecules has been detected and is close to the temperature of the atoms. This technique and similar techniques will be very important for the production and study of cold molecules.

E. Optical Lattices

In 1968 V.S. Letokhov [67] suggested that it is possible to confine atoms in the wavelength size regions of a standing wave by means of the dipole-force that arises from the light shift. This was first accomplished in 1987 in one dimension with an atomic beam traversing an intense standing wave [68]. Since then, the study of atoms confined in wavelength-size potential wells has become an important topic in optical control of atomic motion because it opens up configurations previously accessible only in condensed matter physics using crystals.

The basic ideas of the quantum mechanical motion of particles in a periodic-potential were laid out in the 1930s with the Kronig-Penney-model and Bloch's-theorem, and optical lattices offer important opportunities for their study. For example, these lattices can be made essentially free of defects with only moderate care in spatially filtering the laser beams to assure a single transverse mode structure. Furthermore, the shape of the potential is exactly known, and doesn't depend on the effect of the crystal field or the ionic energy level scheme. Finally, the laser parameters can be varied to modify the depth of the potential wells without changing the lattice vectors, and the lattice vectors can be changed independently by redirecting the laser beams. The simplest optical lattice to consider is a 1D pair of counterpropagating beams of the same polarization, as was used in the first experiment [68].

Because of the transverse nature of light, any mixture of beams with different $\vec{k}$-vectors necessarily produces a spatially periodic, inhomogeneous light field. The importance of the "egg-crate" array of potential wells arises because the associated atomic light-shifts can easily be

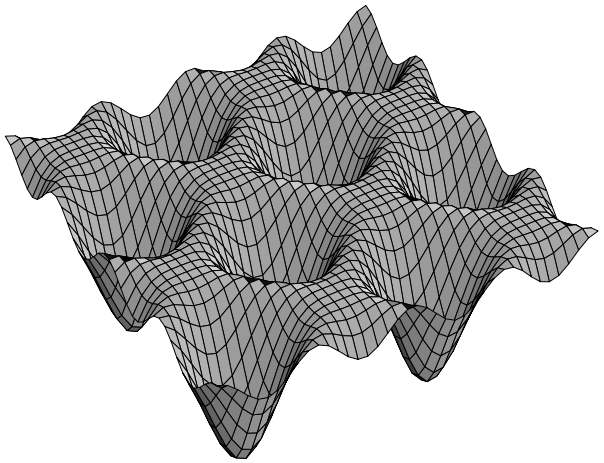

FIG. 17: The 'egg-crate" potential of an optical lattice shown in two dimensions. The potential wells are separated by $\lambda/2$.

comparable to the very low average atomic kinetic energy of laser-cooled atoms. A typical example projected against two dimensions is shown in Fig. 17.

The name "optical lattice" is used rather than optical-crystal because the filling fraction of the lattice sites is typically only a few percent (as of 1999). The limit arises because the loading of atoms into the lattice is typically done from a sample of trapped and cooled atoms, such as a MOT for atom collection, followed by an optical molasses for laser cooling. The atomic-density in such experiments is limited to a few times $10^{11}/\mathrm{cm}^3$ by collisions and multiple light scattering. Since the density of lattice sites of size $\lambda/2$ is a few times $10^{13}/\mathrm{cm}^3$, the filling fraction is necessarily small.

At first thought it would seem that a rectangular 2D or 3D optical lattice could be readily constructed from two or three mutually perpendicular standing waves [69, 70]. However, a sub-wavelength movement of a mirror caused by a small vibration could change the relative phase of the standing waves. In 1993 a very clever scheme was described [71]. It was realized that an n-dimensional lattice could be created by only $n+1$ traveling waves rather than $2n$. Instead of producing optical wells in 2D with four beams (two standing waves), these authors used only three. The $\vec{k}$-vectors of the co-planar beams were separated by $2\pi/3$, and they were all linearly polarized in their common plane (not parallel to one another) The same immunity to vibrations was established for a 3D optical lattice by using only four beams arranged in a quasi-tetrahedral configuration. The three linearly polarized beams of the 2D arrangement described above were directed out of the plane toward a common vertex, and a fourth circularly polarized beam was added. All four beams were polarized in the same plane [71]. The authors showed that such a configuration produced the desired potential wells in 3D.

The NIST group studied atoms loaded into an optical lattice using Bragg-diffraction of laser light from the spatially ordered array [72]. They cut off the laser beams that formed the lattice, and before the atoms had time to move away from their positions, they pulsed on a probe laser beam at the Bragg angle appropriate for one of the sets of lattice planes. The Bragg diffraction not only enhanced the reflection of the probe beam by a factor of 10^5, but by varying the time between the shut-off of the lattice and turn-on of the probe, they could measure the "temperature" of the atoms in the lattice. The reduction of the amplitude of the Bragg scattered beam with time provided some measure of the diffusion of the atoms away from the lattice sites, much like the Debye-Waller-factor in X-ray-diffraction.

Laser cooling has brought the study of the motion of atoms into an entirely new domain where the quantum mechanical nature of their center-of-mass motion must be considered [1]. Such exotic behavior for the motion of whole atoms, as opposed to electrons in the atoms, has not been considered before the advent of laser cooling simply because it is too far out of the range of ordinary experiments. A series of experiments in the early 1990s provided dramatic evidence for these new quantum states of motion of neutral atoms, and led to the debut of de-Broglie wave atom optics.

The limits of laser cooling discussed in section **??** suggest that atomic momenta can be reduced to a "few" times $\hbar k$. This means that their deBroglie wavelengths are equal to the optical wavelengths divided by a "few". If the depth of the optical potential wells is high enough to contain such very slow atoms, then their motion in potential wells of size $\lambda/2$ must be described quantum mechanically, since they are confined to a space of size comparable to their deBroglie wavelengths. Thus they do not oscillate in the sinusoidal wells as classical localizable particles, but instead occupy discrete, quantum mechanical bound states, as shown in the lower part of Fig. 18.

The group at NIST also developed a new method that superposed a weak probe beam of light directly from the laser upon some of the fluorescent light from the atoms in a 3D optical molasses, and directed the light from these combined sources onto on a fast photodetector [73]. The resulting beat signal carried information about the Doppler-shifts of the atoms in the optical lattices [36]. These Doppler shifts were expected to be in the sub-MHz range for atoms with the previously measured 50 μK temperatures. The observed features confirmed the quantum nature of the motion of atoms in the wavelength-size potential wells (see Fig. 19) [19].

In the 1930s Bloch realized that applying a uniform force to a particle in a periodic potential would not accelerate it beyond a certain speed, but instead would result in Bragg-reflection when its deBroglie wavelength became equal to the lattice period. Thus an electric field applied to a conductor could not accelerate electrons to a speed faster than that corresponding to the edge of a Brillouin-zone, and that at longer times the particles would execute oscillatory motion. Ever since then, experimen-

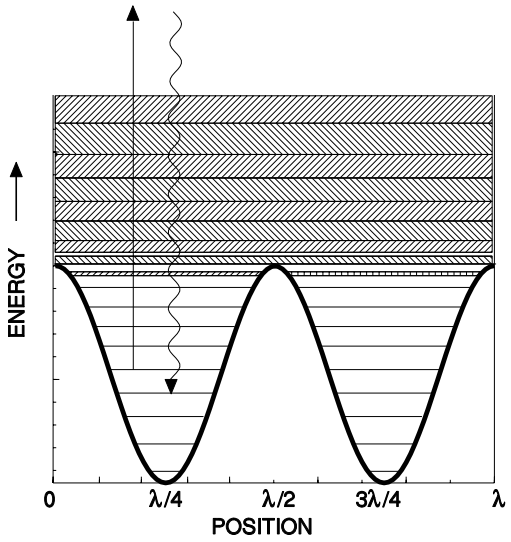

FIG. 18: Energy levels of atoms moving in the periodic potential of the light shift in a standing wave. There are discrete bound states deep in the wells that broaden at higher energy, and become bands separated by forbidden energies above the tops of the wells. Under conditions appropriate to laser cooling, optical pumping among these states favors populating the lowest ones as indicated schematically by the arrows.

talists have tried to observe these Bloch-oscillations in increasingly pure and/or defect-free crystals.

Atoms moving in optical lattices are ideally suited for such an experiment, as was beautifully demonstrated in 1996 [74]. The authors loaded a 1D lattice with atoms from a 3D molasses, further narrowed the velocity distribution, and then instead of applying a constant force, simply changed the frequency of one of the beams of the 1D lattice with respect to the other in a controlled way, thereby creating an accelerating lattice. Seen from the atomic reference frame, this was the equivalent of a constant force trying to accelerate them. After a variable time t_a the 1D lattice beams were shut off and the measured atomic velocity distribution showed beautiful Bloch-oscillations as a function of t_a. The centroid of the very narrow velocity distribution was seen to shift in velocity space at a constant rate until it reached $v_r = \hbar k/M$, and then it vanished and reappeared at $-v_r$ as shown in Fig. 20. The shape of the "dispersion curve" allowed measurement of the "effective mass" of the atoms bound in the lattice.

F. Bose-Einstein Condensation

In 1924 S. Bose found the correct way to evaluate the distribution of identical entities, such as Planck's radiation quanta, that allowed him to calculate the Planck-spectrum using the methods of statistical mechanics. Within a year Einstein had seized upon this idea, and generalized it to identical particles with discrete energies. This distribution is

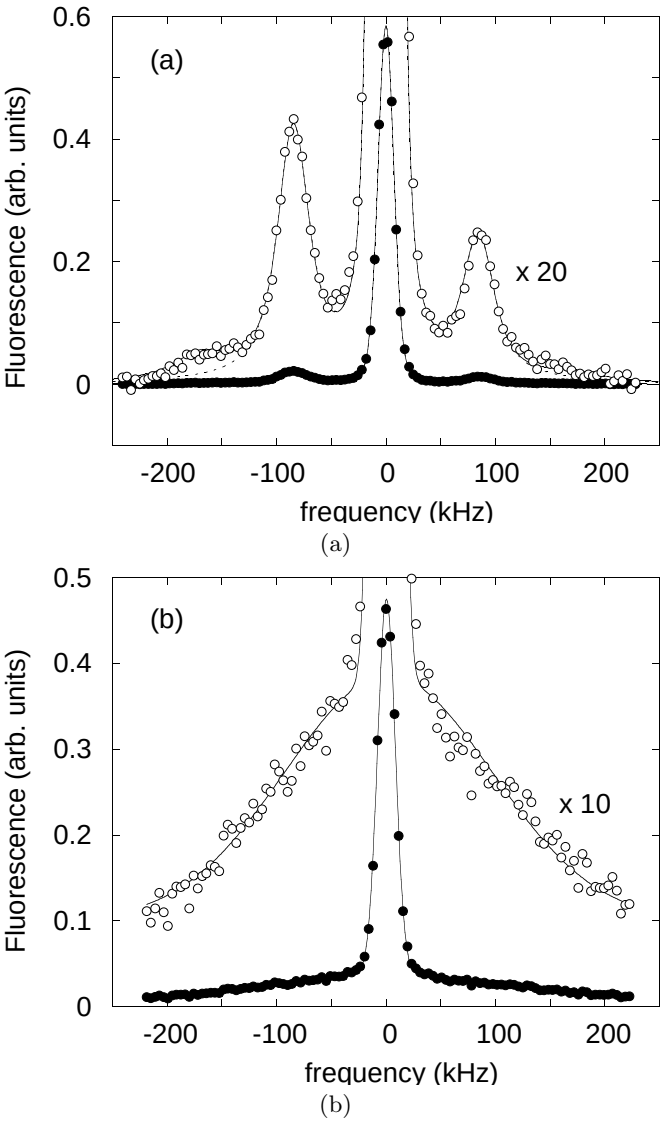

FIG. 19: (a) Fluorescence spectrum in a 1D lin ⊥ lin optical molasses. Atoms are first captured and cooled in an MOT, then the MOT light beams are switched off leaving a pair of lin ⊥ lin beams. Then the measurements are made with $\delta = -4\gamma$ at low intensity. (b) Same as (a) except the 1D molasses is σ^+-σ^- which has no spatially dependent light shift and hence no vibrational motion (figure from Ref. [36]).

$$N(E) = \frac{1}{e^{\beta(E-\mu)} - 1}, \tag{33}$$

where $\beta \equiv 1/k_B T$ and μ is the chemical potential that vanishes for photons: Eq. 33 with $\mu = 0$ is exactly the Planck distribution. Einstein observed that this distribution has the peculiar property that for sufficiently low average energy (*i.e.*, low temperature), the total energy could be minimized by having a discontinuity in the distribution for the population of the lowest allowed state.

The condition for this Bose-Einstein condensation

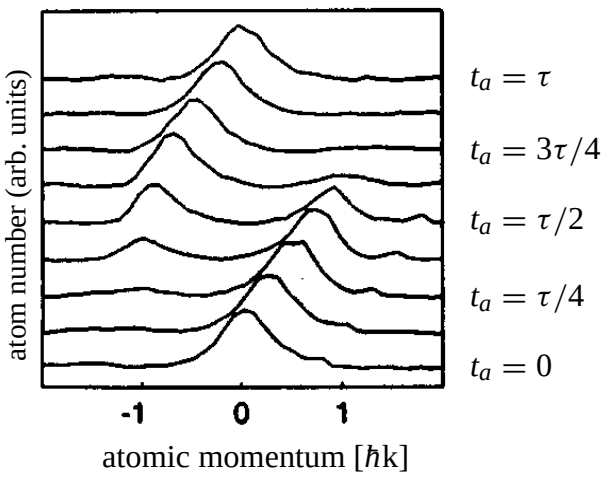

(a)

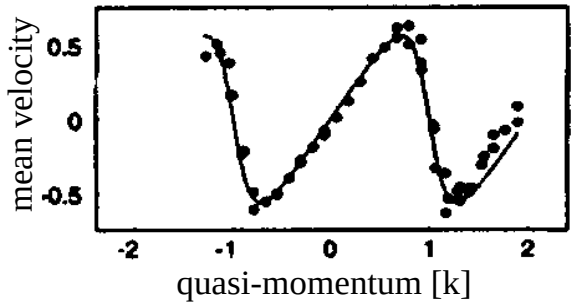

(b)

FIG. 20: Plot of the measured velocity distribution *vs.* time in the accelerated 1D lattice. The atoms accelerate only to the edge of the Brillouin zone where the velocity is $+v_r$, and then the velocity distribution appears at $-v_r$ (figure from Ref. [74]).

(BEC) in a gas can be expressed in terms of the de-Broglie wavelength λ_{dB} associated with the thermal motion of the atoms as $n\lambda_{dB}^3 \geq 2.612\ldots$, where n is the spatial density of the atoms. In essence, this means that the atomic wave functions must overlap one another.

The most familiar elementary textbook description of BEC focuses on non-interacting particles. However, particles *do* interact and the lowest order approximation that is widely used to account for the interaction takes the form of a mean-field repulsive force. It is inserted into the Hamiltonian for the motion of each atom in the trap (*n.b.*, not for the internal structure of the atom) as a term $V_{\rm int}$ proportional to the local density of atoms. Since this local density is itself $|\Psi|^2$, it makes the Schrödinger equation for the atomic motion non-linear, and the result bears the name "Gross-Pitaevski-equation". For N atoms in the condensate it is written

$$\left[-\frac{\hbar^2}{2M}\nabla^2_{\vec{R}} + V_{\rm trap}(\vec{R}) + NV_{\rm int}|\Psi(\vec{R})|^2\right]\Psi(\vec{R}) = E_N\Psi(\vec{R}), \tag{34}$$

where $\vec{R}$ is the coordinate of the atom in the trap, $V_{\rm trap}(\vec{R})$ is the potential associated with the trap that confines the atoms in the BEC, and $V_{\rm int} \equiv 4\pi\hbar^2 a/M$ is the coefficient associated with strength of the mean field interaction between the atoms. Here a is the scattering length (see section VIII D), and M is the atomic mass.

For $a > 0$ the interaction is repulsive so that a BEC would tend to disperse. This is manifest for a BEC confined in a harmonic trap by having its wavefunction somewhat more spread out and flatter than a Gaussian. By contrast, for $a < 0$ the interaction is attractive and the BEC eventually collapses. However, it has been shown that there is metastability for a sufficiently small number of particles with $a < 0$ in a harmonic trap, and that a BEC can be observed in vapors of atoms with such negative scattering length as ^{7}Li [75–77]. This was initially somewhat controversial.

Solutions to this highly non-linear equation 34, and the ramifications of those solutions, form a major part of the theoretical research into BEC. Note that the condensate atoms all have exactly the same wavefunction, which means that adding atoms to the condensate does not increase its volume, just like the increase of atoms to the liquid phase of a liquid-gas mixture makes only an infinitesimal volume increase of the sample. The consequences of this predicted condensation are indeed profound. For example, in a harmonic trap, the lowest state's wavefunction is a Gaussian. With so many atoms having *exactly* the same wavefunction they form a new state of matter, unlike anything in the familiar experience.

Achieving the conditions required for BEC in a low-density atomic vapor requires a long and difficult series of cooling steps. First, note that an atomic sample cooled to the recoil limit T_r would need to have a density of a few times 10^{13} atoms/cm^3 in order to satisfy BEC. However, atoms can not be optically cooled at this density because the resulting vapor would have an absorption length for on-resonance radiation approximately equal to the optical wavelength. Furthermore collisions between ground and excited state atoms have such a large cross section, that at this density the optical cooling would be extremely ineffective. In fact, the practical upper limit to the atomic density for laser cooling in a 3D optical molasses (see Sec. VI B) or MOT (see Sec. VII D) corresponds to $n \sim 10^{10}$ atoms/cm^3. Thus it is clear that the final stage of cooling toward a BEC must be done in the dark. The process typically begins with a MOT for efficient capture of atoms from a slowed beam or from the low-velocity tail of a Maxwell-Boltzmann distribution of atoms at room temperature. Then a polarization gradient optical-molasses stage is initiated that cools the atomic sample from the mK temperatures of the MOT to a few times T_r. For the final cooling stage, the cold atoms are confined in the dark in a purely magnetic-trap and a forced evaporative-cooling process is used to cool [1].

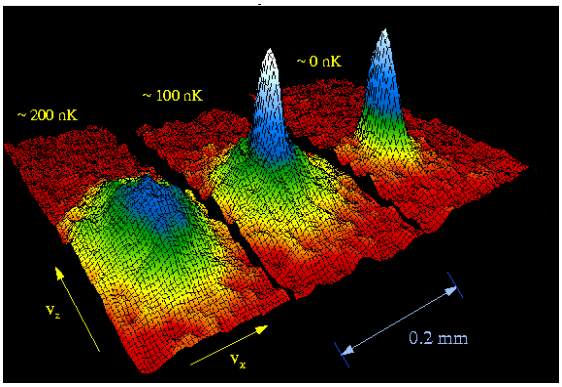

FIG. 21: Three panels showing the spatial distribution of atoms after release from the magnetostatic trap following various degrees of evaporative cooling. In the first one, the atoms were cooled to just before the condition for BEC was met, in the second one, to just after this condition, and in the third one to the lowest accessible temperature consistent with leaving some atoms still in the trap (figure taken from the JILA web page).

The observation of BEC in trapped alkali atoms in 1995 has been the largest impetus to research in this exciting field. As of this writing (1999), the only atoms that have been condensed are Rb [78], Na [79], Li [80], and H [81]. The case of Cs is special because, although BEC is certainly possible, the presence of a near-zero energy resonance severely hampers its evaporative cooling rate.

The first observations of BEC were in Rb [78], Li [80], and Na [79], and the observation was done with ballistic-techniques. The results from one of the first experiments are shown in Fig. 21. The three panels show the spatial distribution of atoms some time after release from the trap. From the ballistic parameters, the size of the BEC sample, as well as its shape and the velocity distribution of its atoms could be inferred. For temperatures too high for BEC, the velocity distribution is Gaussian but asymmetrical. For temperatures below the transition to BEC, the distribution is also not symmetrical, but now shows the distinct peak of a disproportionate number of very slow atoms corresponding to the ground state of the trap from which they were released. As the temperature is lowered further, the number of atoms in the narrow feature increases very rapidly, a sure signature that this is truly a BEC and not just very efficient cooling.

The study of this "new form" of matter has spawned innumerable sub-topics, and has attracted enormous interest. Both theorists and experimentalists are addressing the questions of its behavior in terms of rigidity, acoustics, coherence, and a host of other properties. Extraction of a coherent beam of atoms from a BEC has been labelled an "atom laser, and will surely open the way for new developments in atom optics [1].

G. Dark States

The BEC discussed above is an example of the importance of quantum effects on atomic motion. It occurs when the atomic deBroglie wavelength λ_{dB} and the interatomic distances are comparable. Other fascinating quantum effects occur when atoms are in the light and λ_{dB} is comparable to the optical wavelength. Some topics connected with optical lattices have already been discussed, and the dark states described here are another important example. These are atomic states that cannot be excited by the light field.

The quantum description of atomic motion requires that the energy of such motion be included in the Hamiltonian. The total Hamiltonian for atoms moving in a light field would then be given by

$$\mathcal{H} = \mathcal{H}_{\rm atom} + \mathcal{H}_{\rm rad} + \mathcal{H}_{\rm int} + \mathcal{H}_{\rm kin}, \qquad (35)$$

where $\mathcal{H}_{\rm atom}$ describes the motion of the atomic electrons and gives the internal atomic energy levels, $\mathcal{H}_{\rm rad}$ is the energy of the radiation field and is of no concern here because the field is not quantized, $\mathcal{H}_{\rm int}$ describes the excitation of atoms by the light field and the concomitant light shifts, and $\mathcal{H}_{\rm kin}$ is the kinetic energy E_k of the motion of the atoms' center of mass. This Hamiltonian has eigenstates of not only the internal energy levels and the atom-laser interaction that connects them, but also of the kinetic energy operator $\mathcal{H}_{\rm kin} \equiv \mathcal{P}^2/2M$. These eigenstates will therefore be labeled by quantum numbers of the atomic states as well as the center of mass momentum p. For example, an atom in the ground state, $|g;\ p\rangle$, has energy $E_g + p^2/2M$ which can take on a continuous range of values.

To see how the quantization of the motion of a two-level atom in a monochromatic field allows the existence of a velocity selective dark state, consider the states of a two-level atom with single internal ground and excited levels, $|g;\ p\rangle$ and $|e;\ p'\rangle$. Two ground eigenstates $|g;\ p\rangle$ and $|g;\ p''\rangle$ are generally not coupled to one another by an optical field except in certain cases. For example, in oppositely propagating light beams (1D) there can be absorption-stimulated emission cycles that connect $|g;\ p\rangle$ to itself or to $|g;\ p \pm 2\rangle$ (in this section, momentum is measured in units of $\hbar k$). The initial and final E_k of the atom differ by $\pm 2(p \pm 1)/M$ so energy-conservation requires $p = \mp 1$ and is therefore velocity selective (the energy of the light field is unchanged by the interaction since all the photons in the field have energy $\hbar\omega_\ell$).

The coupling of these two degenerate states by the light field produces off-diagonal matrix elements of the total Hamiltonian $\mathcal{H}$ of Eq. 35, and subsequent diagonalization of it results in the new ground eigenstates of $\mathcal{H}$ given by (see Fig. 22) $|\pm\rangle \equiv (|g;\ -1\rangle \pm |g;\ +1\rangle)/\sqrt{2}$. The excitation rate of these eigenstates $|\pm\rangle$ to $|e;\ 0\rangle$ is proportional to the square of the electric dipole matrix element $\vec{\mu}$ given by

$$|\langle e;\ 0|\vec{\mu}|\pm\rangle|^2 = |\langle e;\ 0|\vec{\mu}|g;\ -1\rangle \pm \langle e;\ 0|\vec{\mu}|g;\ +1\rangle|^2/2. \qquad (36)$$

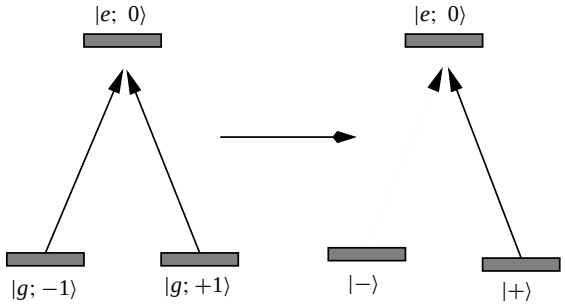

FIG. 22: Schematic diagram of the transformation of the eigenfunctions from the internal atomic states $|g;\ p\rangle$ to the eigenstates $|\pm\rangle$. The coupling between the two states $|g;\ p\rangle$ and $|g;\ p''\rangle$ by Raman transitions mixes them, and since they are degenerate, the eigenstates of $\mathcal{H}$ are the non-degenerate states $|\pm\rangle$.

This vanishes for $|-\rangle$ because the two terms on the right-hand side of Eq. 36 are equal since $\vec{\mu}$ does not operate on the external momentum of the atom (dotted line of Fig. 22). Excitation of $|\pm\rangle$ to $|e;\ \pm 2\rangle$ is much weaker since it's off resonance because its energy is higher by $4\hbar\omega_r = 2\hbar^2k^2/M$, so that the required frequency is higher than to $|e;\ 0\rangle$. The resultant detuning is $4\omega_r = 8\epsilon(\gamma/2)$, and for $\epsilon \sim 0.5$, this is large enough so that the excitation rate is small, making $|-\rangle$ quite dark. Excitation to any state other than $|e;\ \pm 2\rangle$ or $|e;\ 0\rangle$ is forbidden by momentum-conservation. Atoms are therefore optically pumped into the dark state $|-\rangle$ where they stay trapped, and since their momentum components are fixed, the result is velocity-selective coherent population trapping (VSCPT).

A useful view of this dark state can be obtained by considering that its components $|g;\ \pm 1\rangle$ have well defined momenta, and are therefore completely delocalized. Thus they can be viewed as waves traveling in opposite directions but having the same frequency, and therefore they form a standing deBroglie wave. The fixed spatial phase of this standing wave relative to the optical standing wave formed by the counterpropagating light beams results in the vanishing of the spatial integral of the dipole transition matrix element so that the state cannot be excited. This view can also help to explain the consequences of p not exactly equal ± 1, where the deBroglie wave would be slowly drifting in space. It is common to label the average of the momenta of the coupled states as the family-momentum, $\wp$, and to say that these states form a *closed-family*, having family momentum $\wp = 0$ [82, 83].

In the usual case of laser cooling, atoms are subject to both a damping force *and* to random impulses arising from the discrete photon momenta $\hbar k$ of the absorbed and emitted light. These can be combined to make a force *vs.* velocity curve as shown in Fig. 23a. Atoms with $\wp \neq 0$ are always subject to the light field that optically pumps them into the dark state and thus produces random impulses as shown in Fig. 23b. There is no damping-force in the most commonly studied case of a real atom, the $J = 1 \rightarrow 1$ transition in He*, because the Doppler and polarization gradient cooling cancel one another as a result of a numerical "accident" for this particular case.

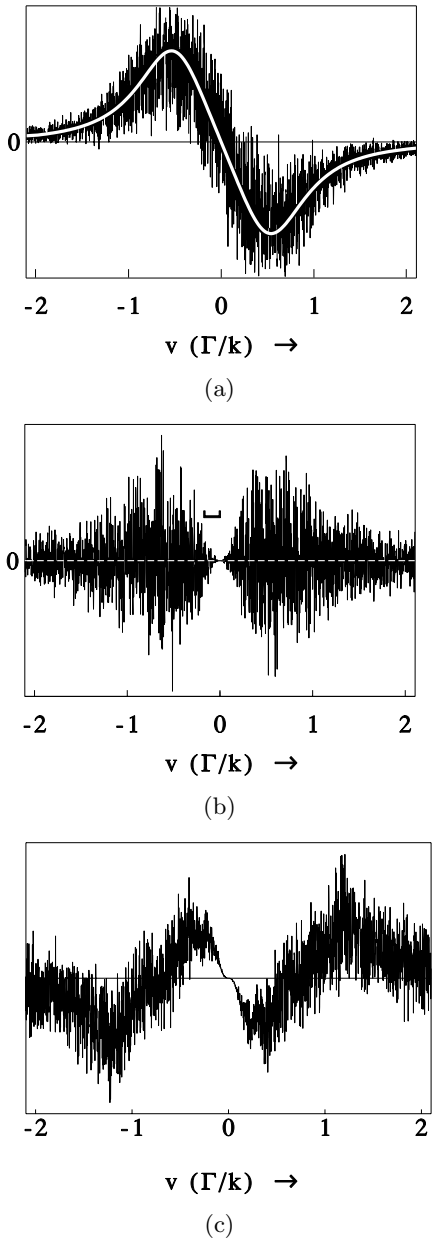

FIG. 23: Calculated force *vs.* velocity curves for different laser configurations showing both the average force and a typical set of simulated fluctuations. Part (a) shows the usual Doppler cooling scheme that produces an atomic sample in steady state whose energy width is $\hbar\gamma/2$. Part (b) shows VSCPT as originally studied in Ref. [82] with no damping force. Note that the fluctuations vanish for $\wp = 0$ because the atoms are in the dark state. Part (c) shows the presence of both a damping force and VSCPT. The fluctuations vanish for $\wp = 0$, and both damping *and* fluctuations are present at $\wp \neq 0$.

Figures 23a and b should be compared to show the velocity dependence of the sum of the damping and random forces for the two cases of ordinary laser cooling and VSCPT. Note that for VSCPT the momentum diffusion vanishes when the atoms are in the dark state at $\wp = 0$, so they can collect there. In the best of both worlds, a damping-force would be combined with VSCPT as shown in Fig. 23c. Such a force was predicted in Ref. [84] and was first observed in 1996 [85].

[1] H.J. Metcalf and P. van der Straten. *Laser Cooling and Trapping*. Springer-Verlag, New York (1999).

[2] J. Gordon and A. Ashkin. Motion of Atoms in a Radiation Trap. *Phys. Rev. A* **21**, 1606 (1980).

[3] W. Phillips and H. Metcalf. Laser Deceleration of an Atomic Beam. *Phys. Rev. Lett.* **48**, 596 (1982).

[4] J. Prodan, W. Phillips, and H. Metcalf. Laser Production of a Very Slow Monoenergetic Atomic Beam. *Phys. Rev. Lett.* **49**, 1149 (1982).

[5] J. Prodan and W. Phillips. Chirping the Light Fantastic — Recent NBS Atom Cooling Experiments. *Prog. Quant. Elect.* **8**, 231 (1984).

[6] W. Ertmer, R. Blatt, J.L.Hall, and M. Zhu. Laser Manipulation of Atomic Beam Velocities: Demonstration of Stopped Atoms and Velocity Reversal. *Phys. Rev. Lett.* **54**, 996 (1985).

[7] R. Watts and C. Wieman. Manipulating Atomic Velocities Using Diode Lasers. *Opt. Lett.* **11**, 291 (1986).

[8] V. Bagnato, G. Lafyatis, A. Martin, E. Raab, R. Ahmad-Bitar, and D. Pritchard. Continuous Stopping and Trapping of Neutral Atoms. *Phys. Rev. Lett.* **58**, 2194 (1987).

[9] T.E. Barrett, S.W. Dapore-Schwartz, M.D. Ray, and G.P. Lafyatis. Slowing Atoms with (σ^-)-Polarized Light. *Phys. Rev. Lett.* **67**, 3483-3487 (1991).

[10] P.A. Molenaar, P. van der Straten, H.G.M. Heideman, and H. Metcalf. Diagnostic-Technique for Zeeman-Compensated Atomic-Beam Slowing — Technique and Results. *Phys. Rev. A* **55**, 605-614 (1997).

[11] J. Dalibard and W. Phillips. Stability and Damping of Radiation Pressure Traps. *Bull. Am. Phys. Soc.* **30**, 748 (1985).

[12] S. Chu, L. Hollberg, J. Bjorkholm, A. Cable, and A. Ashkin. Three-Dimensional Viscous Confinement and Cooling of Atoms by Resonance Radiation Pressure. *Phys. Rev. Lett.* **55**, 48 (1985).

[13] P.D. Lett, R.N. Watts, C.E. Tanner, S.L. Rolston, W.D. Phillips, and C.I. Westbrook. Optical Molasses. *J. Opt. Soc. Am. B* **6**, 2084-2107 (1989).

[14] D. Sesko, C. Fan, and C. Wieman. Production of a Cold Atomic Vapor Using Diode-Laser Cooling. *J. Opt. Soc. Am. B* **5**, 1225 (1988).

[15] B. Sheehy, S.Q. Shang, P. van der Straten, and H. Metcalf. Collimation of a Rubidium Beam Below the Doppler Limit. *Chem. Phys.* **145**, 317-325 (1990).

[16] P. Gould, P. Lett, and W.D. Phillips. New Measurement with Optical Molasses. In W. Persson and S. Svanberg, editors, *Laser Spectroscopy VIII*, page 64, Berlin (1987). Springer.

[17] T. Hodapp, C. Gerz, C. Westbrook, C. Furtlehner, and W. Phillips. Diffusion in Optical Molasses. *Bull. Am. Phys. Soc.* **37**, 1139 (1992).

[18] C. Cohen-Tannoudji and W.D. Phillips. New Mechanisms for Laser Cooling. *Phys. Today* **43**, October, 33-40 (1990).

[19] P. Lett, R. Watts, C. Westbrook, W. Phillips, P. Gould, and H. Metcalf. Observation of Atoms Laser Cooled below the Doppler Limit. *Phys. Rev. Lett.* **61**, 169 (1988).

[20] J. Dalibard and C. Cohen-Tannoudji. Laser Cooling Below the Doppler Limit by Polarization Gradients — Simple Theoretical-Models. *J. Opt. Soc. Am. B* **6**, 2023-2045 (1989).

[21] P.J. Ungar, D.S. Weiss, S. Chu, and E. Riis. Optical Molasses and Multilevel Atoms — Theory. *J. Opt. Soc. Am. B* **6**, 2058-2071 (1989).

[22] C. Salomon, J. Dalibard, W.D. Phillips, A. Clairon, and S. Guellati. Laser Cooling of Cesium Atoms Below 3 μK. *Europhys. Lett.* **12**, 683-688 (1990).

[23] W. Ketterle and N.J. van Druten. Evaporative Cooling of Trapped Atoms. *Adv. Atom. Mol. Opt. Phys.* **37**, 181 (1996).

[24] M. Kasevich and S. Chu. Laser Cooling Below a Photon Recoil with 3-Level Atoms. *Phys. Rev. Lett.* **69**, 1741-1744 (1992).

[25] D. Wineland, W. Itano, J. Bergquist, and J. Bollinger. Trapped Ions and Laser Cooling. Technical Report 1086, N.I.S.T. (1985).

[26] A. Migdall, J. Prodan, W. Phillips, T. Bergeman, and H. Metcalf. First Observation of Magnetically Trapped Neutral Atoms. *Phys. Rev. Lett.* **54**, 2596 (1985).

[27] T. Bergeman, G. Erez, and H. Metcalf. Magnetostatic Trapping Fields for Neutral Atoms. *Phys. Rev. A* **35**, 1535 (1987).

[28] A. Ashkin. Acceleration and Trapping of Particles by Radiation Pressure. *Phys. Rev. Lett.* **24**, 156 (1970).

[29] S. Chu, J. Bjorkholm, A. Ashkin, and A. Cable. Experimental Observation of Optically Trapped Atoms. *Phys. Rev. Lett.* **57**, 314 (1986).

[30] A. Ashkin. Application of Laser Radiation Pressure. *Science* **210**, 1081-1088 (1980).

[31] A. Ashkin and J.M. Dziedzic. Observation of Radiation-Pressure Trapping of Particles by Alternating Light Beams. *Phys. Rev. Lett.* **54**, 1245 (1985).

[32] A. Ashkin and J.M. Dziedzic. Optical Trapping and Manipulation of Viruses and Bacteria. *Science* **235**, 1517 (1987).

[33] J.D. Miller, R.A. Cline, and D.J. Heinzen. Far-Off-Resonance Optical Trapping of Atoms. *Phys. Rev. A* **47**, R4567-R4570 (1993).

[34] Y. Castin and J. Dalibard. Quantization of Atomic Motion in Optical Molasses. *Europhys. Lett.* **14**, 761-766 (1991).

[35] P. Verkerk, B. Lounis, C. Salomon, C. Cohen-Tannoudji, J.Y. Courtois, and G. Grynberg. Dynamics and Spatial Order of Cold Cesium Atoms in a Periodic Optical-Potential. *Phys. Rev. Lett.* **68**, 3861-3864 (1992).

[36] P.S. Jessen, C. Gerz, P.D. Lett, W.D. Phillips, S.L. Rolston, R.J.C. Spreeuw, and C.I. Westbrook. Observation of Quantized Motion of Rb Atoms in an Optical-Field. *Phys. Rev. Lett.* **69**, 49-52 (1992).

[37] B. Lounis, P. Verkerk, J.Y. Courtois, C. Salomon, and G. Grynberg. Quantized Atomic Motion in 1D Cesium Molasses with Magnetic-Field. *Europhys. Lett.* **21**, 13-17 (1993).

[38] E. Raab, M. Prentiss, A. Cable, S. Chu, and D. Pritchard. Trapping of Neutral-Sodium Atoms with Radiation Pressure. *Phys. Rev. Lett.* **59**, 2631 (1987).

[39] T. Walker, D. Sesko, and C. Wieman. Collective Behavior of Optically Trapped Neutral Atoms. *Phys. Rev. Lett.* **64**, 408-411 (1990).

[40] D.W. Sesko, T.G. Walker, and C.E. Wieman. Behavior of Neutral Atoms in a Spontaneous Force Trap. *J. Opt. Soc. Am. B* **8**, 946-958 (1991).

[41] E. Riis, D.S. Weiss, K.A. Moler, and S. Chu. Atom Funnel for the Production of a Slow, High-Density Atomic-Beam. *Phys. Rev. Lett.* **64**, 1658-1661 (1990).

[42] A. Scholz, M. Christ, D. Doll, J. Ludwig, and W. Ertmer. Magneto-optical Preparation of a Slow, Cold and Bright Ne* Atomic-Beam. *Opt. Commun.* **111**, 155-162 (1994).

[43] M.D. Hoogerland, J.P.J. Driessen, E.J.D. Vredenbregt, H.J.L. Megens, M.P. Schuwer, H.C.W. Beijerinck, and K.A.H. van Leeuwen. Bright Thermal Atomic-Beams by Laser Cooling — A 1400-Fold Gain in-Beam Flux. *App. Phys. B* **62**, 323-327 (1996).

[44] Z.T. Lu, K.L. Corwin, M.J. Renn, M.H. Anderson, E.A. Cornell, and C.E. Wieman. Low-Velocity Intense Source of Atoms from a Magnetooptical Trap. *Phys. Rev. Lett.* **77**, 3331-3334 (1996).

[45] K.G.H. Baldwin. private communication.

[46] M. Schiffer, M. Christ, G. Wokurka, and W. Ertmer. Temperatures Near the Recoil Limit in an Atomic Funnel. *Opt. Commun.* **134**, 423-430 (1997).

[47] F. Lison, P. Schuh, D. Haubrich, and D. Meschede. High Brilliance Zeeman Slowed Cesium Atomic Beam. (submitted to App. Phys. B).

[48] K. Dieckmann, R.J.C. Spreeuw, M. Weidemüller, and J.T.M. Walraven. Two-Dimensional Magneto-Optical Trap as a Source of Slow Atoms. *Phys. Rev. A* **58**, 3891 (1998).

[49] J. Nellessen, J.H. Muller, K. Sengstock, and W. Ertmer. Laser Preparation of a Monoenergetic Sodium Beam. *Europhys. Lett.* **9**, 133-138 (1989).

[50] J. Nellessen, J.H. Muller, K. Sengstock, and W. Ertmer. Large-Angle Beam Deflection of a Laser-Cooled Sodium Beam. *J. Opt. Soc. Am. B* **6**, 2149-2154 (1989).

[51] J. Nellessen, J. Werner, and W. Ertmer. Magnetooptical Compression of a Monoenergetic Sodium Atomic-Beam. *Opt. Commun.* **78**, 300-308 (1990).

[52] A. Aspect, N. Vansteenkiste, R. Kaiser, H. Haberland, and M. Karrais. Preparation of a Pure Intense Beam of Metastable Helium by Laser Cooling. *Chem. Phys.* **145**, 307-315 (1990).

[53] R. A. Nauman and H. Henry Stroke. Apparatus Upended: A Short History of the Fountain A-Clock. *Phys. Today* pages May, 89 (1996).

[54] M.A. Kasevich, E. Riis, S. Chu, and R.G. Devoe. RF Spectroscopy in an Atomic Fountain. *Phys. Rev. Lett.* **63**, 612-616 (1989).

[55] A. Clairon, C. Salomon, S. Guellati, and W.D. Phillips. Ramsey Resonance in a Zacharias Fountain. *Europhys. Lett.* **16**, 165-170 (1991).

[56] K. Gibble and S. Chu. Future Slow-Atom Frequency Standards. *Metrologia* **29**, 201-212 (1992).

[57] K. Gibble and S. Chu. Laser-Cooled Cs Frequency Standard and a Measurement of the Frequency-Shift Due to Ultracold Collisions. *Phys. Rev. Lett.* **70**, 1771-1774 (1993).

[58] K. Gibble and B. Verhaar. Eliminating Cold-Collision Frequency Shifts. *Phys. Rev. A* **52**, 3370 (1995).

[59] R. Legere and K. Gibble. Quantum Scattering in a Juggling Atomic Fountain. *Phys. Rev. Lett.* **81**, 5780 (1998).

[60] Ph. Laurent, P. Lemonde, E. Simon, G. Santorelli, A. Clairon, N. Dimarcq, P. Petit, C. Audoin, and C. Salomon. A Cold Atom Clock in the Absence of Gravity. *Eur. Phys. J. D* **3**, 201 (1998).

[61] P.S. Julienne and F.H. Mies. Collisions of Ultracold Trapped Atoms. *J. Opt. Soc. Am. B* **6**, 2257-2269 (1989).

[62] P.D. Lett, P.S. Julienne, and W. D. Phillips. Photoassociative Spectroscopy of Laser-Cooled Atoms. *Annu. Rev. Phys. Chem.* **46**, 423 (1995).

[63] A. Gallagher and D.E. Pritchard. Exoergic Collisions of Cold Na*-Na. *Phys. Rev. Lett.* **63**, 957-960 (1989).

[64] P.S. Julienne and J. Vigue. Cold Collisions of Ground-State and Excited-State Alkali-Metal Atoms. *Phys. Rev. A* **44**, 4464-4485 (1991).

[65] H. Mastwijk, J. Thomsen, P. van der Straten, and A. Niehaus. Optical Collisions of Cold, Metastable Helium Atoms. *Phys. Rev. Lett.* **80**, 5516-5519 (1998).

[66] A. Fioretti, D. Comparat, A. Crubellier, O. Dulieu, F. Masnou-Seeuws, and P. Pillet. Formation of Cold Cs_2 Molecules through Photoassociation. *Phys. Rev. Lett.* **80**, 4402-4405 (1998).

[67] V.S. Lethokov. Narrowing of the Doppler Width in a Standing Light Wave. *JETP Lett.* **7**, 272 (1968).

[68] C. Salomon, J. Dalibard, A. Aspect, H. Metcalf, and C. Cohen-Tannoudji. Channeling Atoms in a Laser Standing Wave. *Phys. Rev. Lett.* **59**, 1659 (1987).

[69] K.I. Petsas, A.B. Coates, and G. Grynberg. Crystallography of Optical Lattices. *Phys. Rev. A* **50**, 5173-5189 (1994).

[70] P.S. Jessen and I.H. Deutsch. Optical Lattices. *Adv. Atom. Mol. Opt. Phys.* **37**, 95-138 (1996).

[71] G. Grynberg, B. Lounis, P. Verkerk, J.Y. Courtois, and C. Salomon. Quantized Motion of Cold Cesium Atoms in 2-Dimensional and 3-Dimensional Optical Potentials. *Phys. Rev. Lett.* **70**, 2249-2252 (1993).

[72] G. Birkl, M. Gatzke, I.H. Deutsch, S.L. Rolston, and W.D. Phillips. Bragg Scattering from Atoms in Optical Lattices. *Phys. Rev. Lett.* **75**, 2823-2826 (1995).

[73] C.I. Westbrook, R.N. Watts, C.E. Tanner, S.L. Rolston, W.D. Phillips, P.D. Lett, and P.L. Gould. Localization of Atoms in a 3-Dimensional Standing Wave. *Phys. Rev. Lett.* **65**, 33-36 (1990).

[74] M. Dahan, E. Peil, J. Reichel, Y. Castin, and C. Salomon. Bloch Oscillations of Atoms in an Optical Potential. *Phys. Rev. Lett.* **76**, 4508 (1996).

[75] H.T.C. Stoof. Atomic Bose-Gas with a Negative Scattering Length. *Phys. Rev. A* **49**, 3824-3830 (1994).

[76] T. Bergeman. Hartree-Fock Calculations of Bose-Einstein Condenstation of ^{7}Li Atoms in a Harmonic Trap for $T > 0$. *Phys. Rev. A* **55**, 3658 (1997).

[77] T. Bergeman. Erratum: Hartree-Fock Calculations of Bose-Einstein Condenstation of ^{7}Li Atoms in a Harmonic Trap for $T > 0$. *Phys. Rev. A* **56**, 3310 (1997).

[78] M.H. Anderson, J.R. Ensher, M.R. Matthews, C.E. Wieman, and E.A. Cornell. Observation of Bose-Einstein Condensation in a Dilute Atomic Vapor. *Science* **269**, 198-201 (1995).

[79] K. Davis, M-O. Mewes, M. Andrews, M. van Druten, D. Durfee, D. Kurn, and W. Ketterle. Bose-Einstein Condensation in a Gas of Sodium Atoms. *Phys. Rev. Lett.* **75**, 3969 (1995).

[80] C.C. Bradley, C.A. Sackett, J.J. Tollett, and R.G. Hulet. Evidence of Bose-Einstein Condensation in an Atomic Gas with Attractive Interactions. *Phys. Rev. Lett.* **75**, 1687-1690 (1995).

[81] D. Fried, T. Killian, L. Willmann, D. Landhuis, S. Moss, D. Kleppner, and T. Greytak. Bose-Einstein Condensation of Atomic Hydrogen. *Phys. Rev. Lett.* **81**, 3811 (1998).

[82] A. Aspect, E. Arimondo, R. Kaiser, N. Vansteenkiste,

and C. Cohen-Tannoudji. Laser Cooling below the One-Photon Recoil Energy by Velocity-Selective Coherent Population Trapping. *Phys. Rev. Lett.* **61**, 826 (1988).

[83] A. Aspect, C. Cohen-Tannoudji, E. Arimondo, N. Vansteenkiste, and R. Kaiser. Laser Cooling Below the One-Photon Recoil Energy by Velocity-Selective Coherent Population Trapping — Theoretical-Analysis. *J. Opt. Soc. Am. B* **6**, 2112-2124 (1989).

[84] M.S. Shahriar, P.R. Hemmer, M.G. Prentiss, P. Marte, J. Mervis, D.P. Katz, N.P. Bigelow, and T. Cai. Continuous Polarization-Gradient Precooling-Assisted Velocity-Selective Coherent Population Trapping. *Phys. Rev. A* **48**, R4035-R4038 (1993).

[85] M. Widmer, M.J. Bellanca, W. Buell, H. Metcalf, M. Doery, and E. Vredenbregt. Measurement of Force-Assisted Population Accumulation in Dark States. *Opt. Lett.* **21**, 606-608 (1996).